Available online at www.sciencedirect.com
SCIENCE DIRECT®
International Journal of Solids and Structures 42 (2005) 5589–5611
INTERNATIONAL JOURNAL OF SOLIDS and STRUCTURES
www.elsevier.com/locate/ijsolstr

A new two-dimensional model for electro-mechanical response of thick laminated piezoelectric actuator

C.W. Lim [a,*], C.W.H. Lau [a,b]

[a] Department of Building and Construction, City University of Hong Kong, Tat Chee Avenue, Kowloon, Hong Kong
[b] Department of Construction, Institute of Vocational Education (Tsing Yi) Tsing Yi, New Territories, Hong Kong

Received 23 February 2005
Available online 13 April 2005

Abstract

This paper investigates the electro-mechanical behaviour of a thick, laminated actuator with piezoelectric and isotropic lamina under externally applied electric loading using a new two-dimensional computational model. The elastic core is relatively thick and thus it is modelled by Timoshenko thick-beam theory. Although the piezoelectric lamina is a beam-like layer, it is formulated via a two-dimensional model because of not only the strong electro-mechanical coupling, but also of the presence of a two-dimensional electric field. It is shown in this paper that a one-dimensional model for the piezoelectric beam-like layer is inadequate. The piezoelectric model is constructed within the scope of linear piezoelectricity. The actuation response is induced through the application of external electric voltage. Under the strong coupling of elasticity and electricity, the strain energy and work of electric potential are presented. The electro-mechanical response of the laminated Timoshenko beam is formulated and determined via a variational energy principle. Numerical examples presented illustrate convincing comparison with finite element solutions and existing published data. New numerical solutions are also presented to investigate the geometric effect on the electro-mechanical bending behaviour.

Keywords: Actuator; Electro-mechanical; Energy method; Piezoelectricity; Laminate

1. Introduction

Piezoelectricity is an electro-mechanical phenomenon which couples elasticity and electricity through the existence of pressure induced electrical field or electric induced stress field. This phenomenon was first discovered by Curie brothers in 1880 (Cady, 1964) and since then, research on piezoelectricity has received

* Corresponding author. Tel.: +852 2788 7285; fax: +852 2788 7612.
E-mail address: bccwlim@cityu.edu.hk (C.W. Lim).

0020-7683/$ - see front matter © 2005 Elsevier Ltd. All rights reserved.
doi:10.1016/j.ijsolstr.2005.02.050

much attention (e.g. Tiersten, 1969; Mason, 1981). Piezoelectric materials have wide range of industrial applications. During the past decade, this material has been used extensively as sensors and/or actuators for controlling vibration, noise and shape of a structural system, and also as the essential component in an accelerometer. In addition, the use of piezoelectric materials as a media to transform electrical and acoustic waves has made telecommunication possible. The advanced micro-electro-mechanical systems (MEMS) use piezoelectric materials in the latest technologies of smart/intelligent designs featuring miniaturization.

One of the practical examples of a piezoelectric device is a piezoelectric accelerometer for triggering the onset of an airbag in tens of thousandths of a second during an accident. The electro-mechanical coupling of piezoelectric materials has immense technological potential in designing smart/intelligent materials and structures ranging from huge aerospace structures to miniatural medical apparatuses. Because of the relative small size and light weight, piezoelectric elements can be integrated in a complex actuator network, such as in robotics design, without significantly affecting the structural properties of the entire system. In order to mobilise piezoelectric effects, the piezoelectric materials are usually surface bonded in patches or fully embedded in the host structure. Hence the structure becomes a laminated piezoelectric actuator. A system with multiple substructures such as a robotic arm may be constituted by a few laminated piezoelectric actuators.

Basic mechanical models for the interaction between an actuator and piezoelectric material have been proposed by many different researchers. As the volume of published papers is large, only relevant and key papers are referenced here. Crawley and de Luis (1987) developed an analytical model with the piezoelectric patches in the beam. They also presented experimental results for their model. Crawley and Anderson (1990) later revised the model based on Euler beam assumption of the displacement function. Tzou and Gadre (1989), Lee (1990), Crawley and Lazarus (1991) developed laminated plate models incorporating the piezoelectric property of materials by using classical laminated theory approximation. Later, Tzou and Zhong (1993) revised the model based on first order shear deformation theory. A very good reference for piezoelectric plate and shell was presented by Tzou (1993). Piezoelectric layers are also frequently used as sensing/actuating elements for control of structures, such as in the postbuckling analysis of thick laminated plates (Shen, 2001) and laminated cylindrical shells (Shen, 2002). Other relevant works include those of Lee and Moon (1989), Wang and Rogers (1991), Koconis et al. (1994a,b), Mitchell and Reddy (1995), Reddy and Mitchell (1995), Saravanos and Heyliger (1995), Batra et al. (1996a,b), Cheng et al. (1999, 2000), He et al. (2000), Lim et al. (2001), Lim and He (2001, 2004), Meguid and Chen (2001), Meguid and Zhao (2002), Cheng and Reddy (2002), He and Lim (2003), Wang and Liew (2003), Liew and Liang (2003), Liew et al. (2003). Recently, Lin et al. (2000) derived an analytic solution of a laminated piezoelectric beam based on the two-dimensional constitutive relationships. Huang and Sun (2001) developed an approximate analytical solutions based on linear piezoelectric and Mindlin lamination theory. Luo and Tong (2002) also developed an exact static solution to smart beams by including peel stresses. Yocum and Abramovich (2002) provided the experimental results on the behaviour of a cantilever beam actuated using piezoelectric patches. A new efficient higher order zigzag theory for composite beams was recently modelled by Kapuria et al. (2003a,b,c, 2004a,b) and it has been successfully applied to many significant engineering problems such as for sandwich piezoelectric beams (Kapuria et al., 2003a), thermal stress analysis (Kapuria et al., 2003b), dynamic analysis (Kapuria et al., 2003c), hybrid piezoelectric beams (Kapuria et al., 2004a) and static loading, buckling, free and forced response of composite and sandwich beams (Kapuria et al., 2004b).

Many of the published papers on piezoelectric laminates considered only thin piezoelectric and elastic layers. However, thick rods or structures with piezoelectric patches exist in many designs such as in the control of robotic arms. Therefore, the mere analysis of thin piezoelectric laminated beams or plates is insufficient in these devices. Although there are certain efforts in three-dimensional analysis of piezoelectric structures (Cheng and Reddy, 2002), the approaches require complicated asymptotic analysis and are somewhat deterrent. In an effort to simplify the analysis, this paper presents an efficient two-dimensional model for the analysis of electro-mechanical response of thick laminated piezoelectric actuators. The piezoelectric model is constructed within the scope of linear piezoelectricity and, therefore, the analysis focuses on low

electric potential differences where such linear piezoelectric constitutive relations are appropriate. Beyond this limit and at high levels of potential difference, especially for moderate to high electric drive inputs for the actuators, hysteresis and nonlinear constitutive relations are inherent to the piezoelectric materials.

Although only electric loading generated by an applied potential difference is considered, the model established in this paper is valid for any combination of mechanical and electrical loadings. Timoshenko beam theory including shear deformation is used to model the thick elastic core. Although the piezoelectric lamina is a beam-like layer, it is formulated via a two-dimensional model because of not only the strong electro-mechanical coupling, but also the presence of a two-dimensional electric field. It is shown in this paper that a one-dimensional model for the piezoelectric beam-like layer is inadequate. A variational energy principle is employed in the modelling of bending strain energy and work of electric potential. Comparison with existing data and finite element solutions are presented to verify the correctness of the approach. Additional new numerical examples are also included to illustrate the effects of geometry and electric field characteristics on the various actuation responses.

2. Formulation of thick laminated actuator

A laminated, cantilever thick actuator of length L and width b is considered. It consists of a thick, elastic core with thickness h_e covered with a piezoelectric layer at the top with thickness h_p as shown in Fig. 1. Hereafter, a subscript e denotes quantities of the elastic core while a subscript p denotes quantities of the piezoelectric layer. The top and bottom surfaces of the laminate are free of shear traction. Two layers of electrode of negligible thickness and negligible stiffness are sandwiched across the piezoelectric layer and an electric potential difference V is applied across the layer. Although the analysis here illustrates a two-layer laminated actuator, it can be easily extended to a multi-layered composite laminate having many piezoelectric layers with various polarization orientations. A rectangular coordinate system (x_1, x_2, x_3) or (x, y, z) is introduced so that the $(x_1, x_2, 0)$-plane coincides with the mid-plane of the elastic core. Referring to this coordinate system, the stress and strain tensors, $\boldsymbol{\sigma}$ and $\boldsymbol{\varepsilon}$, the displacement, electric field and electric displacement vectors, $\mathbf{u}$, $\mathbf{E}$ and $\mathbf{D}$, are denoted according to the usual Voigt's notation, in turn, by

$$\begin{aligned}
\boldsymbol{\sigma} &= [\,\sigma_{11} \quad \sigma_{22} \quad \sigma_{33} \quad \sigma_{23} \quad \sigma_{13} \quad \sigma_{12}\,]^{\mathrm{T}} = [\,\sigma_1 \quad \sigma_2 \quad \sigma_3 \quad \sigma_4 \quad \sigma_5 \quad \sigma_6\,]^{\mathrm{T}},\\
\boldsymbol{\varepsilon} &= [\,\varepsilon_{11} \quad \varepsilon_{22} \quad \varepsilon_{33} \quad 2\varepsilon_{23} \quad 2\varepsilon_{13} \quad 2\varepsilon_{12}\,]^{\mathrm{T}} = [\,\varepsilon_1 \quad \varepsilon_2 \quad \varepsilon_3 \quad \varepsilon_4 \quad \varepsilon_5 \quad \varepsilon_6\,]^{\mathrm{T}},\\
\mathbf{u} &= [\,u_1 \quad u_2 \quad u_3\,]^{\mathrm{T}},\\
\mathbf{E} &= -[\,\varphi_{,1} \quad \varphi_{,2} \quad \varphi_{,3}\,]^{\mathrm{T}},\\
\mathbf{D} &= [\,D_1 \quad D_2 \quad D_3\,]^{\mathrm{T}},
\end{aligned} \tag{1}$$

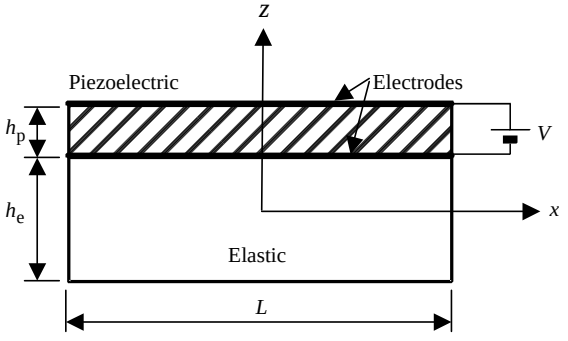

Fig. 1. Laminated thick piezoelectric actuator.

where φ is electric potential, T stands for transpose, and a comma refers to partial differentiation with respect to the suffix variable. Using the usual notation, the infinitesimal strain components are related to the displacement components by

$$\varepsilon_{ij} = \frac{1}{2}(u_{i,j} + u_{j,i}), \tag{2}$$

where lower case Latin indices take the value of 1, 2 or 3, and two repeated indices imply summation.

For simplicity, the piezoelectric element in the laminate is assumed to be poled along the positive direction of x_3, and possess the material symmetry of 6 mm, i.e. the material is transversely isotropic (Tzou, 1993). The case of more general material symmetry can also be considered via the present method, but for brevity the analysis will not be given here. In the scope of linear piezoelectricity, the constitutive relations can be written as (Nye, 1976)

$$\boldsymbol{\sigma} = \mathbf{C}\boldsymbol{\varepsilon} - \mathbf{e}^{\mathrm{T}}\mathbf{E}, \quad \mathbf{D} = \mathbf{e}\boldsymbol{\varepsilon} + \boldsymbol{\kappa}\mathbf{E}, \tag{3}$$

where $\mathbf{C}$, $\mathbf{e}$ and $\boldsymbol{\kappa}$, being 6×6, 3×6 and 3×3 matrices, stand for the elasticity, piezoelectricity and dielectricity tensors as presented in Appendix A. Under quasi-static conditions, the stress and electric displacement satisfy the following equilibrium equations,

$$\sigma_{ij,j} = 0, \quad D_{i,i} = 0. \tag{4}$$

In accordance with the variational energy principle (Reddy, 1984; Tzou, 1993), we define an energy functional Π as the difference of the total strain energy of the structure, $U = U_{\mathrm{e}} + U_{\mathrm{p}}$, and the work done by an external electric potential, W_{p}, as

$$\Pi = U_{\mathrm{e}} + U_{\mathrm{p}} - W_{\mathrm{p}}, \tag{5}$$

where U_{e} and U_{p} are respectively the strain energy of the elastic core and piezoelectric layer. The strain energy of the piezoelectric layer can be expressed as

$$U_{\mathrm{p}} = \int\int\int_{V_{\mathrm{p}}} \frac{1}{2}(\boldsymbol{\varepsilon}^{\mathrm{T}}\boldsymbol{\sigma} - \mathbf{D}^{\mathrm{T}}\mathbf{E})_{\mathrm{p}}\,\mathrm{d}V_{\mathrm{p}} = \int\int\int_{V_{\mathrm{p}}} \left(\frac{1}{2}\boldsymbol{\varepsilon}^{\mathrm{T}}\mathbf{C}\boldsymbol{\varepsilon} - \boldsymbol{\varepsilon}^{\mathrm{T}}\mathbf{e}^{\mathrm{T}}\mathbf{E} - \frac{1}{2}\mathbf{E}^{\mathrm{T}}\boldsymbol{\kappa}\mathbf{E}\right)_{\mathrm{p}} \mathrm{d}V_{\mathrm{p}}, \tag{6}$$

where V_{p} is the volume of piezoelectric layer. For the elastic core, there is no piezoelectric and dielectric effect, i.e. $\mathbf{e} = 0$ and $\boldsymbol{\kappa} = 0$, and its strain energy retains only the first term of Eq. (6), as

$$U_{\mathrm{e}} = \int\int\int_{V_{\mathrm{e}}} \left(\frac{1}{2}\boldsymbol{\varepsilon}^{\mathrm{T}}\mathbf{C}\boldsymbol{\varepsilon}\right)_{\mathrm{e}} \mathrm{d}V_{\mathrm{e}}, \tag{7}$$

where V_{e} is the volume of elastic core. For the laminate, the work done by the applied electric potential is

$$W_{\mathrm{p}} = \int\int_{S_{\mathrm{p}}} \left(\frac{1}{2}\bar{Q}\varphi\right)_{\mathrm{p}} \mathrm{d}S_{\mathrm{p}}, \tag{8}$$

where S_{p} is the area of surface with applied electric potential and $\bar{Q}_{\mathrm{p}}$ is surface charge per unit area of the piezoelectric layer.

Because the elastic core is a thick structure, the Timoshenko beam model is adopted here. In this model, all plane sections originally perpendicular to the longitudinal mid-axis remain plane, but not necessarily perpendicular to the axis after deformation. Hereafter, we use x and z to indicate coordinates in the x_1- and x_3-axes, respectively. For such a thick structure, strain quantities related to the x_2-axis (or y-axis) vanish. The displacement components of the elastic core can be represented as

$$\begin{aligned} u_{\mathrm{e}}(x,z) &= z\theta_{\mathrm{e}}(x), \\ w_{\mathrm{e}}(x,z) &= w_{\mathrm{e}}(x), \end{aligned} \tag{9}$$

where $\theta_e(x)$ and $w_e(x)$ are rotation and transverse displacement of the mid-axis of the elastic core, respectively, and they are only functions depending on x. The strain components can be related to the displacement and rotation of mid-axis as

$$(\varepsilon_1)_e = \frac{\partial u_e}{\partial x} = z\frac{d\theta_e}{dx}; \quad (\varepsilon_5)_e = \left(\frac{\partial u_e}{\partial z} + \frac{\partial w_e}{\partial x}\right) = \left(\theta_e + \frac{dw_e}{dx}\right). \tag{10}$$

For an elastic core made of isotropic material, the relevant elastic constants are

$$(c_{11})_e = E; \quad (c_{55})_e = \kappa^2 G, \tag{11}$$

where E, G are Young's modulus and shear modulus, respectively, and κ^2 is the shear correction factor (Reissner, 1945; Mindlin, 1951) of the elastic core. Introducing dimensionless coordinates $\bar{x} = x/L$, $\bar{z} = z/L$ and dimensionless displacement components $\bar{u}_e = u_e/L$, $\bar{w}_e = w_e/L$ which are normalized with respect to length L, the strain energy of the elastic core as given in Eq. (7) is

$$U_e = \int\int\int_{V_e} \frac{1}{2}\left(\begin{bmatrix}\varepsilon_1\\ \varepsilon_5\end{bmatrix}^T \begin{bmatrix}c_{11} & 0\\ 0 & c_{55}\end{bmatrix}\begin{bmatrix}\varepsilon_1\\ \varepsilon_5\end{bmatrix}\right)_e dV_e = \frac{bL^2}{2}\int\int_{\bar{A}_e}\left[E\left(\frac{\partial \bar{u}_e}{\partial \bar{x}}\right)^2 + \kappa^2 G\left(\frac{\partial \bar{u}_e}{\partial \bar{z}} + \frac{\partial \bar{w}_e}{\partial \bar{x}}\right)^2\right] d\bar{x}\, d\bar{z}, \tag{12}$$

where V_e is volume of elastic core, b is width and $\bar{A}_e$ is normalized area in the $\bar{x}\bar{z}$-plane. Hence, substituting Eq. (9) into Eq. (12) yields

$$\begin{aligned} U_e &= \frac{bL^2}{2}\int_{-0.5}^{0.5}\int_{-\bar{h}_e/2}^{\bar{h}_e/2}\left[E\bar{z}^2\left(\frac{d\theta_e}{d\bar{x}}\right)^2 + \kappa^2 G\left(\theta_e + \frac{d\bar{w}_e}{d\bar{x}}\right)^2\right] d\bar{z}\, d\bar{x} \\ &= \frac{bh_eLE}{2}\int_{-0.5}^{0.5}\left[\frac{h_e^2}{12L^2}\left(\frac{d\theta_e}{d\bar{x}}\right)^2 + \frac{\kappa^2 G}{E}\left(\theta_e + \frac{d\bar{w}_e}{d\bar{x}}\right)^2\right] d\bar{x}, \end{aligned} \tag{13}$$

where $\bar{h}_e = h_e/L$ is the normalized thickness of elastic core.

For the piezoelectric layer, strain, displacement and electric quantities in the x- and z-axes must be retained. For such a piezoelectric layer, the displacement components $u_p(x,z)$ and $w_p(x,z)$ are functions of x and z while the electric potential $\varphi_p(z)$ is only dependent on z due to symmetry of the applied potential and electric boundary conditions, i.e. $(E_1)_p = (E_2)_p = 0$. Using the expressions of elastic, piezoelectric and dielectric constants in Appendix A, the strain energy of piezoelectric layer as given in Eq. (6) can be expressed as

$$\begin{aligned} U_p &= \int\int\int_{V_p}\left\{\frac{1}{2}\begin{bmatrix}\varepsilon_1\\ \varepsilon_3\\ \varepsilon_5\end{bmatrix}^T\begin{bmatrix}c_{11} & c_{13} & 0\\ c_{13} & c_{33} & 0\\ 0 & 0 & c_{55}\end{bmatrix}\begin{bmatrix}\varepsilon_1\\ \varepsilon_3\\ \varepsilon_5\end{bmatrix} - \begin{bmatrix}\varepsilon_1\\ \varepsilon_3\\ \varepsilon_5\end{bmatrix}^T\begin{bmatrix}c & e_{31}\\ 0 & e_{33}\\ e_{15} & 0\end{bmatrix}\begin{bmatrix}E_1\\ E_3\end{bmatrix} - \frac{1}{2}\begin{bmatrix}E_1\\ E_3\end{bmatrix}^T\begin{bmatrix}k_{11} & 0\\ 0 & k_{33}\end{bmatrix}\begin{bmatrix}E_1\\ E_3\end{bmatrix}\right\}_p dV \\ &= \int\int\int_{V_p}\left\{\frac{1}{2}\left[c_{11}\varepsilon_1^2 + 2c_{13}\varepsilon_1\varepsilon_3 + c_{33}\varepsilon_3^2 + c_{55}\varepsilon_5^2\right] - e_{31}\varepsilon_1 E_3 - e_{33}\varepsilon_3 E_3 - \frac{1}{2}k_{33}E_3^2\right\}_p dV, \end{aligned} \tag{14}$$

where

$$(\varepsilon_1)_p = \frac{\partial u_p}{\partial x}, \quad (\varepsilon_3)_p = \frac{\partial w_p}{\partial z}, \quad (\varepsilon_5)_p = \frac{\partial u_p}{\partial z} + \frac{\partial w_p}{\partial x}, \quad (E_3)_p = -\frac{\partial \varphi_p}{\partial z}. \tag{15}$$

Substituting Eqs. (15) into Eq. (14), integrating over width b and normalizing the quantities and coordinate system yield

$$U_{\mathrm{p}} = bL^2 \int\int_{\bar{A}_{\mathrm{p}}} \left\{ \frac{c_{11}}{2}\left(\frac{\partial \bar{u}_{\mathrm{p}}}{\partial \bar{x}}\right)^2 + c_{13}\frac{\partial \bar{u}_{\mathrm{p}}}{\partial \bar{x}}\frac{\partial \bar{w}_{\mathrm{p}}}{\partial \bar{z}} + \frac{c_{33}}{2}\left(\frac{\partial \bar{w}_{\mathrm{p}}}{\partial \bar{z}}\right)^2 + \frac{c_{55}}{2}\left[\left(\frac{\partial \bar{u}_{\mathrm{p}}}{\partial \bar{z}}\right)^2 + 2\left(\frac{\partial \bar{u}_{\mathrm{p}}}{\partial \bar{z}}\frac{\partial \bar{w}_{\mathrm{p}}}{\partial \bar{x}}\right) + \left(\frac{\partial \bar{w}_{\mathrm{p}}}{\partial \bar{x}}\right)^2\right] + \frac{e_{31}V}{L}\frac{\partial \bar{u}_{\mathrm{p}}}{\partial \bar{x}}\frac{\partial \bar{\varphi}_{\mathrm{p}}}{\partial \bar{z}} + \frac{e_{33}V}{L}\frac{\partial \bar{w}_{\mathrm{p}}}{\partial \bar{z}}\frac{\partial \bar{\varphi}_{\mathrm{p}}}{\partial \bar{z}} - \frac{k_{33}}{2}\frac{V^2}{L^2}\left(\frac{\partial \bar{\varphi}_{\mathrm{p}}}{\partial \bar{z}}\right)^2 \right\} \mathrm{d}\bar{x}\,\mathrm{d}\bar{z}, \tag{16}$$

where $\bar{u}_{\mathrm{p}} = u_{\mathrm{p}}/L$, $\bar{w}_{\mathrm{p}} = w_{\mathrm{p}}/L$ are the dimensionless displacement components and $\bar{\varphi}_{\mathrm{p}} = \varphi_{\mathrm{p}}/V$ is the normalized electric potential.

Integrating the work of applied electric in Eq. (8) over the top area with applied potential using the same normalized coordinate system yield

$$W_{\mathrm{p}} = \frac{1}{2}Q\ \varphi_{\mathrm{p}}\Big|_{\bar{z}=\bar{h}_{\mathrm{e}}/2}^{\bar{z}=\bar{h}_{\mathrm{e}}/2+\bar{h}_{\mathrm{p}}} = \frac{1}{2}QV, \tag{17}$$

where $Q = bL\bar{Q}$ is total surface charge, $\bar{h}_{\mathrm{p}} = h_{\mathrm{p}}/L$ is the normalized thickness of piezoelectric layer and $\varphi_{\mathrm{p}}\big|_{\bar{z}=\bar{h}_{\mathrm{e}}/2}^{\bar{z}=\bar{h}_{\mathrm{e}}/2+\bar{h}_{\mathrm{p}}} = V$ is the potential difference across the two electrodes. Substituting Eqs. (13), (16) and (17) into Eq. (5) results in an energy functional as

$$\Pi = \frac{bh_{\mathrm{e}}LE}{2}\int_{-0.5}^{0.5}\left[\frac{h_{\mathrm{e}}^2}{12L^2}\left(\frac{\mathrm{d}\theta_{\mathrm{e}}}{\mathrm{d}\bar{x}}\right)^2 + \frac{\kappa^2 G}{E}\left(\theta_{\mathrm{e}} + \frac{\mathrm{d}\bar{w}_{\mathrm{e}}}{\mathrm{d}\bar{x}}\right)^2\right]\mathrm{d}\bar{x} + bL^2\int\int_{\bar{A}_{\mathrm{p}}}\left\{\frac{c_{11}}{2}\left(\frac{\partial \bar{u}_{\mathrm{p}}}{\partial \bar{x}}\right)^2 + c_{13}\frac{\partial \bar{u}_{\mathrm{p}}}{\partial \bar{x}}\frac{\partial \bar{w}_{\mathrm{p}}}{\partial \bar{z}} + \frac{c_{33}}{2}\left(\frac{\partial \bar{w}_{\mathrm{p}}}{\partial \bar{z}}\right)^2 + \frac{c_{55}}{2}\left[\left(\frac{\partial \bar{u}_{\mathrm{p}}}{\partial \bar{z}}\right)^2 + 2\left(\frac{\partial \bar{u}_{\mathrm{p}}}{\partial \bar{z}}\frac{\partial \bar{w}_{\mathrm{p}}}{\partial \bar{x}}\right) + \left(\frac{\partial \bar{w}_{\mathrm{p}}}{\partial \bar{x}}\right)^2\right] + \frac{e_{31}V}{L}\frac{\partial \bar{u}_{\mathrm{p}}}{\partial \bar{x}}\frac{\partial \bar{\varphi}_{\mathrm{p}}}{\partial \bar{z}} + \frac{e_{33}V}{L}\frac{\partial \bar{w}_{\mathrm{p}}}{\partial \bar{z}}\frac{\partial \bar{\varphi}_{\mathrm{p}}}{\partial \bar{z}} - \frac{k_{33}}{2}\frac{V^2}{L^2}\left(\frac{\partial \bar{\varphi}_{\mathrm{p}}}{\partial \bar{z}}\right)^2\right\}\mathrm{d}\bar{x}\,\mathrm{d}\bar{z} - \frac{1}{2}QV. \tag{18}$$

3. Boundary conditions and continuity conditions

In using the variational energy method described in the next section, the model needs to satisfy the geometric and electric boundary conditions at the edges, and the geometric and electric continuity conditions at the interface. For a cantilever actuator, one end is fixed at $\bar{x} = -0.5$ while the other at $\bar{x} = 0.5$ is free, as shown in Fig. 1. Therefore all displacement components at the fixed end must be zero, as

$$\bar{u}_{\mathrm{e}} = \bar{w}_{\mathrm{e}} = \bar{u}_{\mathrm{p}} = \bar{w}_{\mathrm{p}} = 0 \quad \text{at } \bar{x} = -0.5 \tag{19}$$

and the gradients of $\bar{w}_{\mathrm{e}}$ and $\bar{w}_{\mathrm{p}}$ must also vanish at the clamped boundary, as

$$\frac{\partial \bar{w}_{\mathrm{e}}}{\partial \bar{x}} = \frac{\partial \bar{w}_{\mathrm{p}}}{\partial \bar{x}} = 0 \quad \text{at } \bar{x} = -0.5. \tag{20}$$

However, there is no strict requirement to satisfy the natural boundary conditions such as vanishing shear force and bending moment at the free end. Numerical investigations showed that the natural boundary conditions are safeguarded if adequate terms are included in the numerical analysis to ensure convergence of numerical solutions.

For a laminated structure, the displacement components must be continuous across the interface. Hence, on the interface at $\bar{z} = \bar{h}_e/2$,

$$\bar{u}_e = \bar{u}_p \quad \text{and } \bar{w}_e = \bar{w}_p. \tag{21}$$

For the piezoelectric layer sandwiched with two electrodes with negligible thickness and stiffness, an electric potential V is applied at the top electrode while of the underneath electrode is earthed. Hence, the electric boundary and interface conditions are

$$\bar{\varphi}_p = 1 \quad \text{at } \bar{z} = \frac{\bar{h}_e}{2} + \bar{h}_p \tag{22a}$$

and

$$\bar{\varphi}_p = 0 \quad \text{at } \bar{z} = \frac{\bar{h}_e}{2}. \tag{22b}$$

4. Admissible functions and nonhomogeneous equation

In the present study, the Ritz method with a variational energy functional is adopted (Reddy, 1984). With reference to the boundary and interface conditions detailed in Section 3, the admissible displacements functions of the elastic and piezoelectric layers can be represented as

$$\bar{u}_e = \bar{z}\theta_e = \bar{z}(\bar{x} + 0.5)\left[C^1_{\theta_e} + C^2_{\theta_e}\bar{x} + C^3_{\theta_e}\bar{x}^2 + C^4_{\theta_e}\bar{x}^3 + \cdots\right] = \bar{z}\sum_{i=1}^{m_e} C^i_{\theta_e}\theta^i_e, \tag{23}$$

$$\bar{w}_e = (\bar{x} + 0.5)^2\left[C^1_{w_e} + C^2_{w_e}\bar{x} + C^3_{w_e}\bar{x}^2 + C^4_{w_e}\bar{x}^3 + \cdots\right] = \sum_{i=1}^{m_e} C^i_{w_e}\bar{w}^i_e, \tag{24}$$

$$\begin{aligned}\bar{u}_p = \bar{u}_e + \bar{u}'_p &= \frac{\bar{h}_e}{2}\theta_e + (\bar{x} + 0.5)\left(\bar{z} - \frac{\bar{h}_e}{2}\right)\left[C^1_{u_p} + C^2_{u_p}\bar{x} + C^3_{u_p}\bar{z} + C^4_{u_p}\bar{x}^2 + C^5_{u_p}\bar{x}\bar{z} + C^6_{u_p}\bar{z}^2 + \cdots\right] \\ &= \frac{\bar{h}_e}{2}\sum_{i=1}^{m_e} C^i_{\theta_e}\theta^i_e + \sum_{i=1}^{m_p} C^i_{u_p}\bar{u}^i_p,\end{aligned} \tag{25}$$

$$\begin{aligned}\bar{w}_p = \bar{w}_e + \bar{w}'_p &= \bar{w}_e + (\bar{x} + 0.5)^2\left(\bar{z} - \frac{\bar{h}_e}{2}\right)\left[C^1_{w_p} + C^2_{w_p}\bar{x} + C^3_{w_p}\bar{z} + C^4_{w_p}\bar{x}^2 + C^5_{w_p}\bar{x}\bar{z} + C^6_{w_p}\bar{z}^2 + \cdots\right] \\ &= \sum_{i=1}^{m_e} C^i_{w_e}\bar{w}^i_e + \sum_{i=1}^{m_p} C^i_{w_p}\bar{w}^i_p,\end{aligned} \tag{26}$$

where m_e and m_p are the number of terms for the displacement components in elastic core and piezoelectric layer, respectively. Similarly, the admissible electric potential function can be approximated as

$$\begin{aligned}\bar{\varphi}_p &= \left(\bar{z} - \frac{\bar{h}_e}{2}\right)\left[\frac{1}{\bar{h}_p} + \left(\bar{z} - \frac{\bar{h}_e}{2} - \bar{h}_p\right)\left(C^1_{\varphi_p} + C^2_{\varphi_p}\bar{z} + C^3_{\varphi_p}\bar{z}^2 + C^4_{\varphi_p}\bar{z}^3 + \cdots\right)\right] \\ &= \left(\bar{z} - \frac{\bar{h}_e}{2}\right)\frac{1}{\bar{h}_p} + \sum_{i=1}^{m_\varphi} C^i_{\varphi_p}\bar{\varphi}^i_p,\end{aligned} \tag{27}$$

where m_φ is the number of terms for the potential function.

Based on the principle of extremum energy, the energy functional in Eq. (18) is minimized with respect to the coefficients, C_α^i $(\alpha = \theta_e, w_e, u_p, w_p, \varphi_p)$, as

$$\frac{\partial \Pi}{\partial C_\alpha^i} = \frac{\partial U_e}{\partial C_\alpha^i} + \frac{\partial U_p}{\partial C_\alpha^i} - \frac{\partial W_p}{\partial C_\alpha^i} = \frac{\partial U_e}{\partial C_\alpha^i} + \frac{\partial U_p}{\partial C_\alpha^i} = 0, \tag{28}$$

since $W_p = \frac{1}{2}QV = \text{constant}$ and $\frac{\partial W_p}{\partial C_\alpha^i} = 0$. Substituting Eqs. (23)–(27) in Eq. (18) and Eq. (28) yields a set of nonhomogeneous equation as

$$[K][C_\alpha] = [T] \tag{29}$$

or

$$\begin{bmatrix} k_{\theta_e\theta_e} & k_{\theta_e w_e} & k_{\theta_e u_p} & k_{\theta_e w_p} & 0 \\ & k_{w_e w_e} & k_{w_e u_p} & k_{w_e w_p} & 0 \\ & & k_{u_p u_p} & k_{u_p w_p} & k_{u_p \varphi_p} \\ & & & k_{w_p w_p} & k_{w_p \varphi_p} \\ \text{sym} & & & & k_{\varphi_p \varphi_p} \end{bmatrix} \begin{Bmatrix} C_{\theta_e} \\ C_{w_e} \\ C_{u_p} \\ C_{w_p} \\ C_{\varphi_p} \end{Bmatrix} = \begin{Bmatrix} t_1 \\ 0 \\ t_3 \\ t_4 \\ 0 \end{Bmatrix}, \tag{30}$$

where $[K]$, $[C_\alpha]$ and $[T]$ are the stiffness matrix, coefficient vector and external load vector, respectively. Expressions of the elements of stiffness matrix are presented in Appendix B. Hence we have a system of linearly independent simultaneous equations for the unknown coefficients which can be solved numerically.

5. Numerical examples of a laminated piezoelectric actuator

A laminated cantilever actuator under an applied potential difference as shown in Fig. 1 is considered. The elastic core is steel and the piezoelectric layer is PZT-4. The material properties are shown in Table 1. A potential difference V is applied to the electrodes across the PZT-4 layer. In the examples, V is varied from 10 V to 40 V to investigate its effect. Moreover, the geometrical effect on the bending behaviour is also investigated.

5.1. Convergence study

A numerical convergence study is carried out to determine the optimal number of terms required in the displacement functions $\bar{u}_e$, $\bar{w}_e$, $\bar{u}_p$, $\bar{w}_p$ and the potential function $\bar{\varphi}_p$. At the beginning, the number of terms

Table 1
Material properties

	Elastic core (steel)	Piezoelectric layer (PZT-4)
Length, m	0.3	0.3
Thickness, m	0.02	0.005
Poisson's ratio	0.3	–
Elastic constants, GPa	$E = 210$	$c_{11} = 139$
		$c_{12} = 77.8$
		$c_{13} = 74.3$
		$c_{33} = 113$
		$c_{44} = 25.6$
Piezoelectric constants, c/m^2		$e_{31} = -6.98$
		$e_{33} = 13.84$
		$e_{15} = 13.44$
Dielectric constants, c/vm		$\kappa_{11} = 6 \times 10^{-9}$
		$\kappa_{33} = 5.47 \times 10^{-9}$

in $\bar{\varphi}_p$ in Eq. (27) is invariant while deflection solutions are determined by varying the number of terms m_e in Eqs. (23) and (24) adopted in $\bar{u}_e$ and $\bar{w}_e$ for the elastic core and m_p in Eqs. (25) and (26) adopted in $\bar{u}_p$ and $\bar{w}_p$ for the PZT-4 layer. Here, Eqs. (23) and (24) involve polynomial $\bar{x}$-terms in an ascending order. For Eqs. (25) and (26), however, we do not adopt a polynomial $\bar{x}\bar{z}$-terms in a complete ascending order because the laminated piezoelectric beam under investigation has a $\bar{x}$-dimension an order higher than the $\bar{z}$-dimension. Only the linear $\bar{z}$-terms are retained while the order of $\bar{x}$-terms are increased. Accordingly, the modified displacement functions for $\bar{u}_p$ and $\bar{w}_p$ involve polynomial terms of the pattern

$$C^1 + C^2\bar{x} + C^3\bar{z} + C^4\bar{x}^2 + C^5\bar{x}\bar{z} + C^6\bar{x}^3 + C^7\bar{x}^2\bar{z} + C^8\bar{x}^4 + C^9\bar{x}^3\bar{z} + C^{10}\bar{x}^5 + C^{11}\bar{x}^4\bar{z}\cdots$$

The choice of such polynomials improves the numerical convergence markedly.

The convergence result is tabulated in Table 2(a) for $V = 10$ V and in Table 2(b) for $V = 40$ V. It is observed that the deflection $\bar{w}_p$ at $\bar{x} = 0.5$ and $\bar{z} = \bar{h}_e/2 + \bar{h}_p$ converges as m_e is increased. The deflection

Table 2
Convergence study for $\bar{w}_p$ at $\bar{x} = 0.5$ and $\bar{z} = \bar{h}_e/2 + \bar{h}_p$ with increasing terms in displacement functions of elastic core m_e, and of piezoelectric layer m_p for $L = 0.3$ m, $h_e = 0.02$ m, $h_p = 0.005$ m and (a) $V = 10$ V, (b) $V = 40$ V

m_p	m_e						
	2	3	4	5	6	7	8
(a)							
3	297.8	300.3	301.6	301.7	301.7	301.7	301.7
4	338.0	342.2	342.5	343.2	343.2	343.2	343.2
5	338.2	342.5	342.7	343.4	343.4	343.4	343.4
6	361.1	362.2	365.7	365.8	366.7	366.7	366.7
7	361.1	364.2	365.8	365.9	366.8	366.8	366.7
8	377.4	379.6	381.0	381.6	381.6	382.1	382.1
9	377.6	379.8	381.1	381.8	381.8	382.3	382.3
10	387.4	389.0	389.9	390.7	390.8	390.8	391.3
11	387.4	389.0	389.9	390.7	390.8	390.8	391.3
12	395.6	396.7	397.3	398.1	398.4	398.5	398.5
13	395.9	397.0	397.6	398.4	398.6	398.7	398.7
14	400.7	401.6	401.9	402.6	402.8	402.9	402.9
15	400.7	401.6	401.9	402.6	402.8	402.9	402.9
16	405.4	406.1	406.2	406.8	407.0	407.2	407.3
17	405.7	406.3	406.5	407.1	407.2	407.4	407.4
18	408.3	408.8	408.9	409.4	409.4	409.7	409.7
(b)							
3	1191	1201	1206	1207	1207	1207	1207
4	1352	1369	1370	1373	1373	1373	1373
5	1353	1370	1371	1374	1374	1374	1374
6	1444	1457	1463	1463	1467	1467	1467
7	1444	1457	1463	1464	1467	1467	1467
8	1510	1518	1524	1527	1526	1528	1528
9	1510	1519	1525	1527	1527	1529	1529
10	1550	1556	1560	1563	1563	1563	1565
11	1550	1556	1560	1563	1563	1563	1565
12	1582	1587	1589	1592	1594	1594	1594
13	1583	1588	1590	1593	1594	1595	1595
14	1603	1606	1608	1610	1611	1612	1612
15	1603	1606	1608	1610	1611	1612	1612
16	1622	1624	1625	1627	1628	1629	1629
17	1623	1625	1626	1628	1629	1630	1630
18	1633	1635	1636	1637	1638	1639	1639

Table 3
Convergence study for $\bar{w}_p$ at $\bar{x} = 0.5$ and $\bar{z} = \bar{h}_e/2 + \bar{h}_p$ with increasing terms in electric potential function of piezoelectric layer m_φ for $L = 0.3$ m, $h_e = 0.02$ m and $h_p = 0.005$ m

Applied voltage, V	m_φ		
	2	3	4
10	381.8	381.8	382.8
40	1572.3	1572.3	1572.3

converges to a relatively steady value when $m_e = 5$. Therefore, $m_e = 5$ is assumed in subsequent calculation unless otherwise stated. Likewise, m_p is also increased gradually to investigate its effect on numerical convergence. It is observed that marked increases in the deflection $\bar{w}_p$ at $\bar{x} = 0.5$ and $\bar{z} = \bar{h}_e/2 + \bar{h}_p$ is only recorded when the order of polynomial (the sum of the powers of $\bar{x}$ and $\bar{y}$) increases. However when $m_p = 19$, numerical ill-conditioning of eigenvalue evaluation occurs. Since satisfactory convergence of $\bar{w}_p$ is observed when there are 18 terms, $m_p = 18$ is assumed in subsequent calculation.

Similar treatment has been used to investigate convergence of the potential function $\bar{\varphi}_p$. In this case, the number of $m_e = 5$ and $m_p = 18$ are maintained while the number of terms for potential function, m_φ in Eq. (27) increases. The results are tabulated in Table 3. It can be observed that $\bar{\varphi}_p$ converges very quickly and only two terms are required to ensure satisfactory convergence. Therefore, the number of terms for $\bar{\varphi}_p$ is chosen as $m_\varphi = 2$.

5.2. Verification of numerical solutions

Having determined numerical convergence, the numerical solutions must be verified in order to ensure accuracy of the approach. Here, we refer to both published data of Lin et al. (2000) and finite element (FE) solutions using ABAQUS (2002), a commercial software package. With reference to Lin et al. (2000), the actuator has $L = 0.3$ m, $h_e = 0.02$ m, $h_p = 0.005$ m and $V = 10$ V.

Lin et al. (2000) derived an analytic solution of the same problem by using constitutive elastic–piezoelectric relationships. They adopted a first order and second order polynomial functions for horizontal and vertical displacement components, respectively. As it has been indicated in Section 5.1 that we require polynomial of order four ($m_e = 5$ terms) for elastic core and polynomial of order nine ($m_p = 18$ terms) for PZT-4 layer to ensure numerical convergence, it is expected that the analysis of Lin et al. (2000) results in a structure which is too stiff and with poor convergence.

In using ABAQUS for FE analysis of the laminated piezoelectric actuator, a technical implementation has to be justified. Here we built a three-dimensional actuator with finite width in the y-dimension. For executing this 3-D actuator in ABAQUS, inputs for all 3-D elastic, piezoelectric and dielectric constants are required. In order to simulate a (x, z) two-dimensional plate-like actuator as shown in Fig. 1, the stiffness in the y-dimension (equivalent to the thickness direction for bending of a plate) is increased to a level such that the strain components in that direction is negligible. This condition is equivalent to the transverse thickness inextensibility restriction for bending of a plate in which transverse deflection through thickness is the same as the transverse deflection of the mid-plane, i.e. the deflection is a constant along the thickness y-direction. It should be indicated that mesh convergence of FE solutions has also been verified. As this is a standard procedure, it is sufficient here only to mention that the mesh has been increased from 360 elements to 7500 steadily in seven steps (360, 525, 900, 1200, 1800, 3400 and 7500) and downward convergent tip deflection solution of the beam has been verified. Further finer meshes result in unstable FE solutions. All subsequent FE solutions are based on a mesh of 7500 elements.

A comparison study is presented in Figs. 2–6. In these figures, the results of Lin et al. (2000), FE solutions and the computational solutions of this paper are compared. Originally, Lin et al. (2000) presented results for the applied potential of 10 V only. Since the study in this paper extended the applied voltage to 40 V, we worked out the results of 40 V from analytical expressions of Lin et al. (2000) which are presented in Figs. 7–11 for comparison.

The dimensional horizontal displacement component u_p of the PZT-4 layer with an applied potential of 10 V along the actuator on the surface at $\bar{z} = \bar{h}_e/2 + \bar{h}_p$ is shown in Fig. 2. In general, u_p in this study

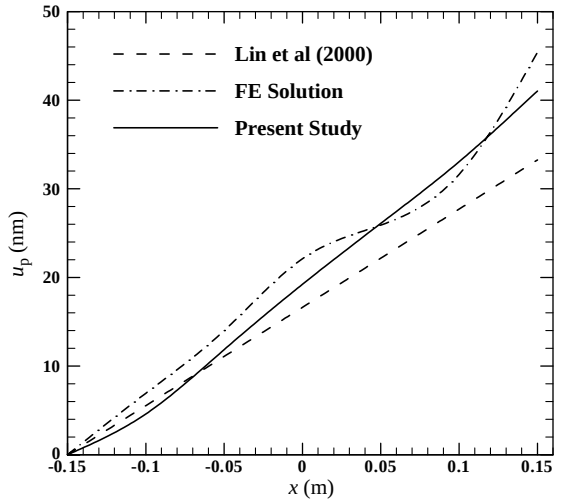

Fig. 2. The displacement u_p of the piezoelectric layer at the actuator free-end $z = h_e/2 + h_p$ with $V = 10$ V.

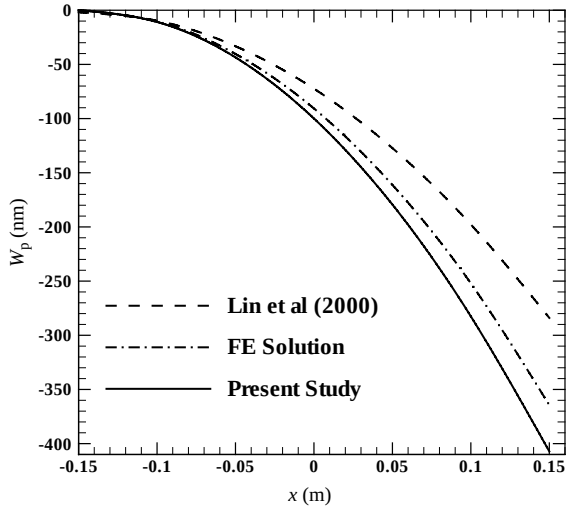

Fig. 3. The displacement w_p of the piezoelectric layer at the actuator free-end $z = h_e/2 + h_p$ with $V = 10$ V.

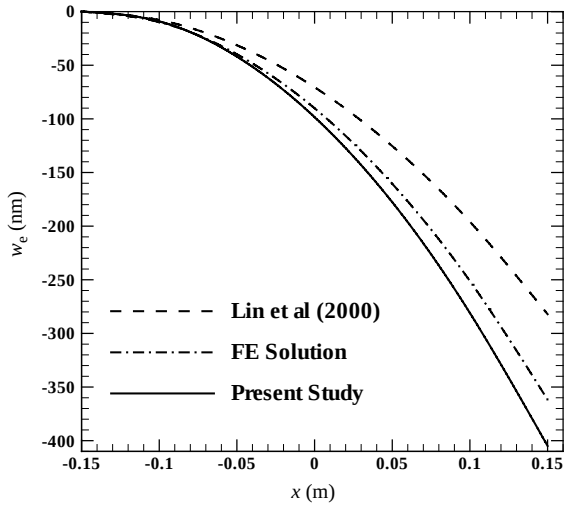

Fig. 4. The displacement w_e of the elastic layer at the actuator free-end $z = 0$ with $V = 10$ V.

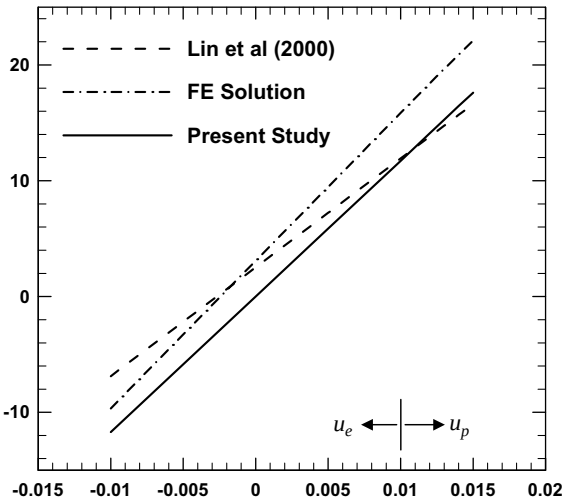

Fig. 5. The displacement u at the mid-span $x = 0$ with $V = 10$ V.

is in better agreement with the FE solution and both are larger than the results of Lin's et al. (2000). It is interesting to observe that the FE solution oscillates from the clamped boundary towards the free boundary. It is due to numerical instability as the magnitude of u_p is of an order smaller than w_p. As explain in Section 5.2, the solution of Lin et al. (2000) is rather poor because a second order polynomial displacement function was used in the study. As concluded in the convergence study, the second order polynomial function has inadequate terms resulting in a stiffer structure and thus smaller displacement as shown in Fig. 2.

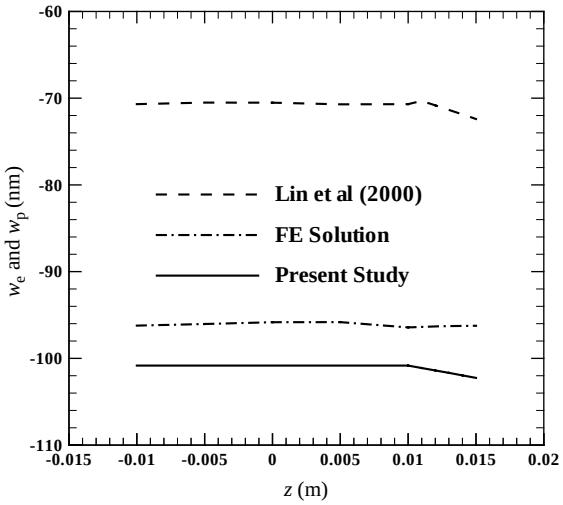

Fig. 6. The displacement w at the mid-span $x = 0$ with $V = 10$ V.

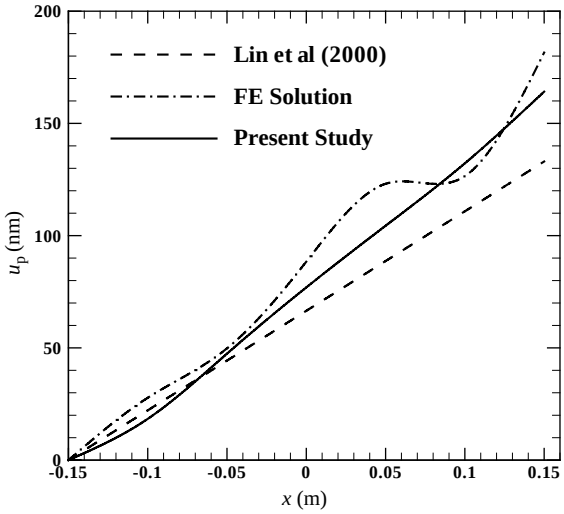

Fig. 7. The displacement u_p of the piezoelectric layer at the actuator free-end $z = h_e/2 + h_p$ with $V = 40$ V.

Figs. 3 and 4 show the vertical displacement components w_e at $\bar{z} = 0$ and w_p at $\bar{z} = \bar{h}_e/2 + \bar{h}_p$ along the actuator for both elastic layer and PZT-4 layer with $V = 10$ V. In both cases, the result of this study is closer to the FE solution and both are, again, larger than that of Lin et al. (2000). For instance, at the free end $x = 0.15$ m of actuator in Fig. 3, the magnitude of w_e is approximately 409 nm and 364 nm according to the analyses in this study and FE, respectively, while it is approximately 280 nm as reported in Lin et al. (2000).

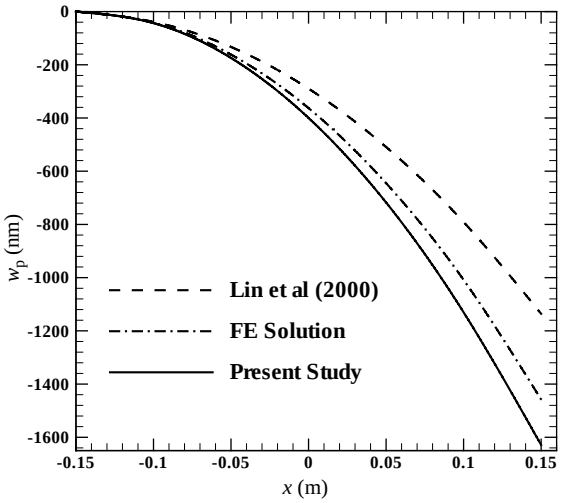

Fig. 8. The displacement w_p of the piezoelectric layer at the actuator free-end $z = h_e/2 + h_p$ with $V = 40$ V.

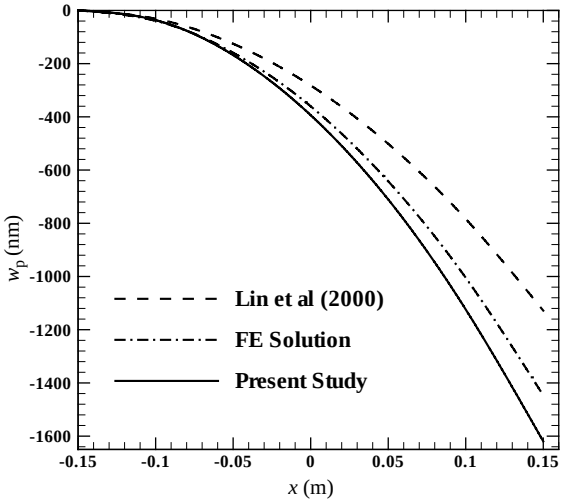

Fig. 9. The displacement w_e of the elastic layer verses x at the actuator free-end $z = 0$ with $V = 40$ V.

Oscillatory response of FE solution does not occur here because w_e and w_p have an-order-higher dominating magnitude over u_p and thus avoiding numerical instability.

Figs. 5 and 6 illustrate the respective vertical and horizontal displacement components u_e and u_p through the thickness along the cross section at the mid-span $\bar{x} = 0$. In both figures, the solutions of this study and FE have the same rate of response and both are larger than the solution of Lin et al. (2000). Again, agreement of the solutions of this study and FE is much better.

The argument above is further verified by examples using a larger applied potential difference of $V = 40$ V. Comparing with Figs. 2–6, it is clear that the results in Figs. 7–11 have similar patterns and comments with respect to those of $V = 10$ V in Figs. 2–6.

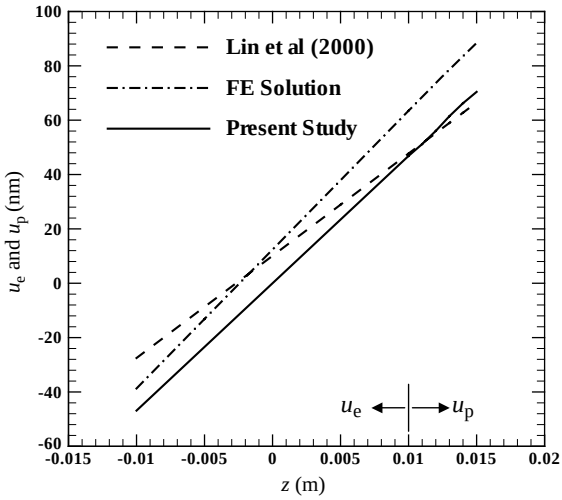

Fig. 10. The displacement components u_e and u_p at the mid-span $x = 0$ with $V = 40$ V.

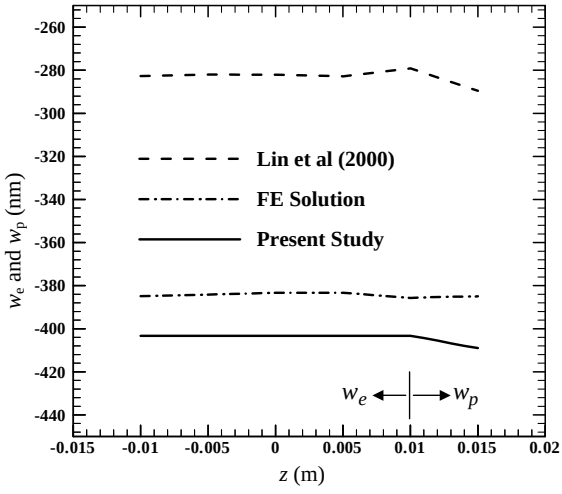

Fig. 11. The displacement components w_e and w_p at mid-span $x = 0$ with $V = 40$ V.

5.3. Effect of electric potential, thickness ratio and length on actuation response

Different actuator geometric configurations based on the same example above are conducted to investigate the effect of the geometric parameters such as dimensionless thickness ratios $\bar{h}_e$ and $\bar{h}_p$ to the response of the laminated actuator. The response is investigated with respect to varying dimensionless potential difference in the range of $V/V_p = \overline{V} = 1$ to $\overline{V} = 4$ where $V_p = 10$ V is a reference potential difference.

As shown in Fig. 12, deflection response $\bar{w}_p$ at $\bar{x} = 0.5$ and $\bar{z} = \bar{h}_e/2 + \bar{h}_p$ is directly proportional to the applied voltage and thus $\overline{V}$ has a linear effect of the structural response. This figure also illustrates the effects of increasing thickness $\bar{h}_p$ of PZT-4 layer from 1/60 to 1/15 while keeping the thickness of elastic core as

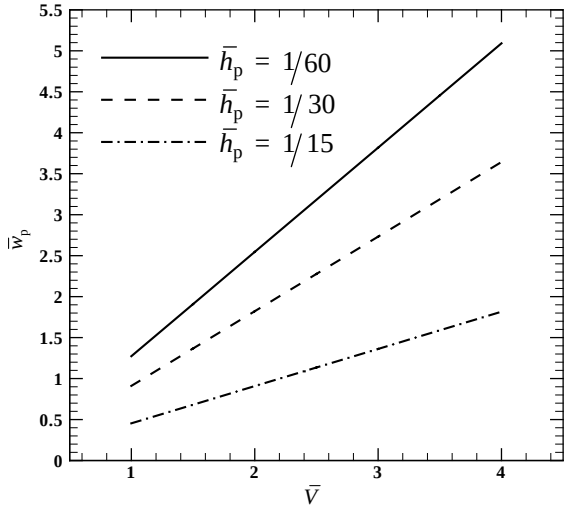

Fig. 12. Effect of thickness ratio $\bar{h}_p$ to the deflection $\bar{w}_p$ at $\bar{x} = 0.5$ and $\bar{z} = \bar{h}_e/2 + \bar{h}_p$.

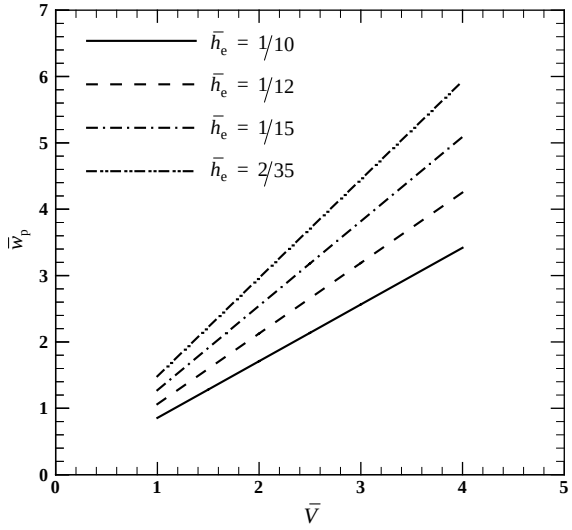

Fig. 13. Effect of the length ratio $\bar{h}_e$ to the deflection $\bar{w}_p$ at $\bar{x} = 0.5$ and $\bar{z} = \bar{h}_e/2 + \bar{h}_p$.

$\bar{h}_e = 1/15$ as that used in Lin et al. (2000). Hence the total thickness of the actuator increases gradually from 1/12 to 2/15. As the stiffness of a structure increases with respect to thickness, $\bar{w}_p$ decreases as $\bar{h}_p$ is increased as shown in Fig. 12.

As illustrated in Fig. 13, varying only the length of actuator L while keeping the thickness h_e constant with the same applied voltage increases the deflection $\bar{w}_p$ at $\bar{x} = 0.5$ and $\bar{z} = \bar{h}_e/2 + \bar{h}_p$. In this case, $\bar{h}_e$ varies from 1/10 to 2/35. The result is obvious since the longer the actuator the more flexible it becomes. In addition, the rate of increase of the deflection to the applied voltage is also larger for a longer actuator. The argument is further verified in Fig. 14. In this case, the applied voltage is constant for each case ranging

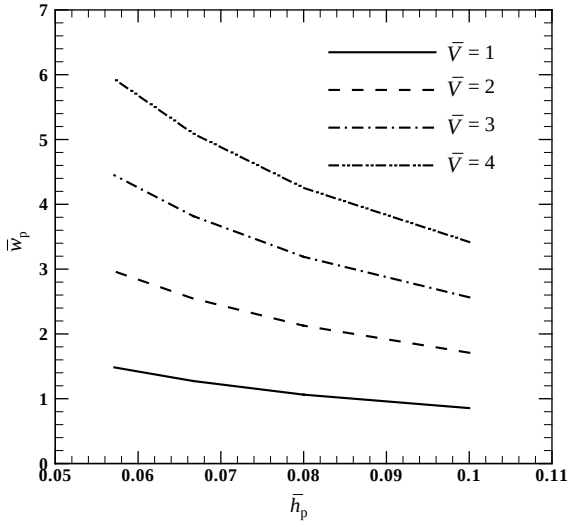

Fig. 14. Effect of applied voltage $\overline{V}$ to the deflection $\bar{w}_p$ at $\bar{x} = 0.5$ and $\bar{z} = \bar{h}_e/2 + \bar{h}_p$.

from $\overline{V} = 1$ to $\overline{V} = 4$. The actuator deflection $\bar{w}_p$ decreases by increasing $\bar{h}_e$ since the actuator becomes shorter and stiffer. The rate of decrease slows down as $\bar{h}_e$ increases.

6. Conclusion

An efficient two-dimensional laminate model is developed to investigate the actuation response of a thick laminated piezoelectric actuator. The piezoelectric model is constructed within the scope of linear piezoelectricity for low electric drive inputs and linear piezoelectric constitutive relations. The presence of hysteresis and nonlinear piezoelectric constitutive relations for high electric drive inputs will form an important extension of this paper.

The piezoelectric laminate model is based on the coupling of a one-dimensional thick layer and a two-dimensional linear piezoelectric layer. The problem is solved via the variational extremum energy principle. Although the model only ensures continuity of displacement across the layer interface, the results from the model are in good agreement with the finite element solutions. The solutions of Lin et al. (2000) are poor because inadequate terms were used in their polynomial displacement functions. This two-dimensional laminate model can be easily and readily developed to investigate a multi-layer piezoelectric laminated actuator.

Numerical results of a thick laminated cantilever actuator under an applied potential difference are discussed. It has been concluded that the electric potential developed across the piezoelectric layer is linear through the thickness. In addition, the deflection response of the actuator is also directly proportional to the applied voltage. The approach and information presented here are of practical interest in engineering control using an actuator. It can also be adapted as a sensor/actuator.

Acknowledgement

The work described in this paper was supported by grants from City University of Hong Kong [Project nos. CityU 1036/01E and 7001534 (BC)].

Appendix A

The matrices **C**, **e** and $\boldsymbol{\kappa}$ in (3) are given as

$$\mathbf{C} = \begin{bmatrix} c_{11} & c_{12} & c_{13} & 0 & 0 & 0 \\ c_{12} & c_{11} & c_{13} & 0 & 0 & 0 \\ c_{13} & c_{13} & c_{33} & 0 & 0 & 0 \\ 0 & 0 & 0 & c_{44} & 0 & 0 \\ 0 & 0 & 0 & 0 & c_{44} & 0 \\ 0 & 0 & 0 & 0 & 0 & c_{66} \end{bmatrix}, \quad \text{where } c_{66} = (c_{11} - c_{12})/2,$$

$$\mathbf{e} = \begin{bmatrix} 0 & 0 & 0 & 0 & e_{15} & 0 \\ 0 & 0 & 0 & e_{15} & 0 & 0 \\ e_{31} & e_{31} & e_{33} & 0 & 0 & 0 \end{bmatrix}, \quad \boldsymbol{\kappa} = \begin{bmatrix} k_{11} & 0 & 0 \\ 0 & k_{11} & 0 \\ 0 & 0 & k_{33} \end{bmatrix}. \tag{A.1}$$

Appendix B

The strain energy of the elastic layer is

$$U_e = \frac{bh_eLE}{2}\int_{-0.5}^{0.5}\left[\frac{h_e^2}{12L^2}\left(\frac{\partial\theta_e}{\partial\bar{x}}\right)^2 + \frac{\kappa^2 G}{E}\left(\theta_e + \frac{\partial\bar{w}_e}{\partial\bar{x}}\right)^2\right]d\bar{x},$$

$$\frac{\partial U_e}{\partial C^i_{\theta_e}} = bh_eLE\int_{-0.5}^{0.5}\left[\frac{h_e^2}{12L^2}\frac{\partial\theta^i_e}{\partial\bar{x}}\frac{\partial\theta_e}{\partial\bar{x}} + \frac{\kappa^2 G}{E}\theta^i_e\left(\theta_e + \frac{\partial\bar{w}_e}{\partial\bar{x}}\right)\right]d\bar{x}$$
$$= bh_eLE\sum_{j=1}^{m}\left[\frac{h_e^2}{12L^2}C^j_{\theta_e}\int_{-0.5}^{0.5}\frac{\partial\theta^i_e}{\partial\bar{x}}\frac{\partial\theta^j_e}{\partial\bar{x}}\,d\bar{x} + \frac{\kappa^2 G}{E}\left(C^j_{\theta_e}\int_{-0.5}^{0.5}\theta^i_e\theta^j_e d\bar{x} + C^j_{w_e}\int_{-0.5}^{0.5}\theta^i_e\frac{\partial\bar{w}^j_e}{\partial\bar{x}}\,d\bar{x}\right)\right],$$

$$\frac{\partial U_e}{\partial C^i_{w_e}} = bh_eLE\int_{-0.5}^{0.5}\left[\frac{\kappa^2 G}{E}\frac{\partial\bar{w}^i_e}{\partial\bar{x}}\left(\theta_e + \frac{\partial\bar{w}_e}{\partial\bar{x}}\right)\right]d\bar{x}$$
$$= bh_eLE\sum_{j=1}^{m}\frac{\kappa^2 G}{E}\left[C^j_{\theta_e}\int_{-0.5}^{0.5}\frac{\partial\bar{w}^i_e}{\partial\bar{x}}\theta^j_e\,d\bar{x} + C^j_{w_e}\int_{-0.5}^{0.5}\frac{\partial\bar{w}^i_e}{\partial\bar{x}}\frac{\partial\bar{w}^j_e}{\partial\bar{x}}\,d\bar{x}\right].$$

The strain energy of the piezoelectric layer is

$$U_p = bL^2\int\int_{\bar{A}_p}\left\{\frac{c_{11}}{2}\left[\frac{h_e^2}{4L^2}\left(\frac{\partial\theta_e}{\partial\bar{x}}\right)^2 + \frac{h_e}{L}\frac{\partial\theta_e}{\partial\bar{x}}\frac{\partial\bar{u}'_p}{\partial\bar{x}} + \left(\frac{\partial\bar{u}'_p}{\partial\bar{x}}\right)^2\right] + c_{13}\left[\frac{h_e}{2L}\frac{\partial\theta_e}{\partial\bar{x}}\frac{\partial\bar{w}'_p}{\partial\bar{z}} + \frac{\partial\bar{u}'_{pu}}{\partial\bar{x}}\frac{\partial\bar{w}'_p}{\partial\bar{z}}\right] + \frac{c_{33}}{2}\left(\frac{\partial\bar{w}'_p}{\partial\bar{z}}\right)^2$$
$$+\frac{c_{55}}{2}\left[\left(\frac{\partial\bar{u}'_p}{\partial\bar{z}}\right)^2 + 2\left(\frac{\partial\bar{u}'_p}{\partial\bar{z}}\frac{\partial\bar{w}_e}{\partial\bar{x}} + \frac{\partial\bar{u}'_p}{\partial\bar{z}}\frac{\partial\bar{w}'_p}{\partial\bar{x}}\right) + \left(\frac{\partial\bar{w}_e}{\partial\bar{x}}\right)^2 + 2\frac{\partial\bar{w}_e}{\partial\bar{x}}\frac{\partial\bar{w}'_p}{\partial\bar{x}} + \left(\frac{\partial\bar{w}'_p}{\partial\bar{x}}\right)^2\right]$$
$$+\frac{e_{31}V}{L}\left[\frac{h_e}{2L}\frac{\partial\theta_e}{\partial\bar{x}}\frac{\partial\bar{\varphi}_p}{\partial\bar{z}} + \frac{\partial\bar{u}'_p}{\partial\bar{x}}\frac{\partial\bar{\varphi}_p}{\partial\bar{z}}\right] + \frac{e_{33}V}{L}\frac{\partial\bar{w}'_p}{\partial\bar{z}}\frac{\partial\bar{\varphi}_p}{\partial\bar{z}} - \frac{k_{33}}{2}\frac{V^2}{L^2}\left(\frac{\partial\bar{\varphi}_p}{\partial\bar{z}}\right)^2\right\}d\bar{x}\,d\bar{z}.$$

$$\frac{\partial U_{\mathrm{p}}}{\partial C^i_{\theta_{\mathrm{e}}}} = bL^2E\frac{h_{\mathrm{e}}}{2L}\left\{\sum_{j=1}^{m}\left[\frac{c_{11}}{E}\left(\frac{h_{\mathrm{e}}}{2L}\frac{h_{\mathrm{p}}}{L}C^j_{\theta_{\mathrm{e}}}\int_{-0.5}^{0.5}\frac{\partial\theta^i_{\mathrm{e}}}{\partial\bar{x}}\frac{\partial\theta^j_{\mathrm{e}}}{\partial\bar{x}}\,\mathrm{d}\bar{x}+C^j_{u_{\mathrm{p}}}\int_{-0.5}^{0.5}\frac{\partial\theta^i_{\mathrm{e}}}{\partial\bar{x}}\int_{h_{\mathrm{e}}/2L}^{h_{\mathrm{e}}/2L+h_{\mathrm{p}}/L}\frac{\partial\bar{u}^j_{\mathrm{p}}}{\partial\bar{x}}\,\mathrm{d}\bar{z}\,\mathrm{d}\bar{x}\right)\right.$$
$$\left.+\frac{c_{13}}{E}C^j_{w_{\mathrm{p}}}\int_{-0.5}^{0.5}\frac{\partial\theta^i_{\mathrm{e}}}{\partial\bar{x}}\left(\bar{w}^j_{\mathrm{p}}\Big|_{\bar{z}=h_{\mathrm{e}}/2L}^{\bar{z}=h_{\mathrm{e}}/2L+h_{\mathrm{p}}/L}\right)\mathrm{d}\bar{x}\right]+\frac{e_{31}V}{EL}\left(\theta^i_{\mathrm{e}}\Big|_{\bar{x}=-0.5}^{\bar{x}=0.5}\right)\right\},$$

$$\frac{\partial U_{\mathrm{p}}}{\partial C^i_{w_{\mathrm{e}}}} = bL^2E\sum_{j=1}^{m}\left[\frac{c_{55}}{E}\left(C^j_{u_{\mathrm{p}}}\int_{-0.5}^{0.5}\frac{\partial\bar{w}^i_{\mathrm{e}}}{\partial\bar{x}}\left(\bar{u}^j_{\mathrm{p}}\Big|_{\bar{z}=h_{\mathrm{e}}/2L}^{\bar{z}=h_{\mathrm{e}}/2L+h_{\mathrm{p}}/L}\right)\mathrm{d}\bar{x}+C^j_{w_{\mathrm{e}}}\frac{h_{\mathrm{p}}}{L}\int_{-0.5}^{0.5}\frac{\partial\bar{w}^i_{\mathrm{e}}}{\partial\bar{x}}\frac{\partial\bar{w}^j_{\mathrm{e}}}{\partial\bar{x}}\,\mathrm{d}\bar{x}\right.\right.$$
$$\left.\left.+C^j_{w_{\mathrm{p}}}\int_{-0.5}^{0.5}\frac{\partial\bar{w}^i_{\mathrm{e}}}{\partial\bar{x}}\int_{h_{\mathrm{e}}/2L}^{h_{\mathrm{e}}/2L+h_{\mathrm{p}}/L}\frac{\partial\bar{w}^j_{\mathrm{p}}}{\partial\bar{x}}\,\mathrm{d}\bar{z}\,\mathrm{d}\bar{x}\right)\right],$$

$$\frac{\partial U_{\mathrm{p}}}{\partial C^i_{u_{\mathrm{p}}}} = bL^2E\left\{\sum_{j=1}^{m}\left[\frac{c_{11}}{E}\left(\frac{h_{\mathrm{e}}}{2L}C^j_{\theta_{\mathrm{e}}}\int_{-0.5}^{0.5}\int_{h_{\mathrm{e}}/2L}^{h_{\mathrm{e}}/2L+h_{\mathrm{p}}/L}\frac{\partial\bar{u}^i_{\mathrm{p}}}{\partial\bar{x}}\,\mathrm{d}\bar{z}\frac{\partial\theta^j_{\mathrm{e}}}{\partial\bar{x}}\,\mathrm{d}\bar{x}+C^j_{u_{\mathrm{p}}}\int_{-0.5}^{0.5}\int_{h_{\mathrm{e}}/2L}^{h_{\mathrm{e}}/2L+h_{\mathrm{p}}/L}\frac{\partial\bar{u}^i_{\mathrm{p}}}{\partial\bar{x}}\frac{\partial\bar{u}^j_{\mathrm{p}}}{\partial\bar{x}}\,\mathrm{d}\bar{z}\,\mathrm{d}\bar{x}\right)\right.\right.$$
$$+\frac{c_{13}}{E}C^j_{w_{\mathrm{p}}}\int_{-0.5}^{0.5}\int_{h_{\mathrm{e}}/2L}^{h_{\mathrm{e}}/2L+h_{\mathrm{p}}/L}\frac{\partial\bar{u}^i_{\mathrm{p}}}{\partial\bar{x}}\frac{\partial\bar{w}^j_{\mathrm{p}}}{\partial\bar{z}}\,\mathrm{d}\bar{z}\,\mathrm{d}\bar{x}+\frac{c_{55}}{E}\left(C^j_{u_{\mathrm{p}}}\int_{-0.5}^{0.5}\int_{h_{\mathrm{e}}/2L}^{h_{\mathrm{e}}/2L+h_{\mathrm{p}}/L}\frac{\partial\bar{u}^i_{\mathrm{p}}}{\partial\bar{z}}\frac{\partial\bar{u}^j_{\mathrm{p}}}{\partial\bar{z}}\,\mathrm{d}\bar{z}\,\mathrm{d}\bar{x}\right.\right.$$
$$\left.+C^j_{w_{\mathrm{e}}}\int_{-0.5}^{0.5}\left(\bar{u}^i_{\mathrm{p}}\Big|_{\bar{z}=h_{\mathrm{e}}/2L}^{\bar{z}=h_{\mathrm{e}}/2L+h_{\mathrm{p}}/L}\right)\frac{\partial\bar{w}^j_{\mathrm{e}}}{\partial\bar{x}}\,\mathrm{d}\bar{x}+C^j_{w_{\mathrm{p}}}\int_{-0.5}^{0.5}\int_{h_{\mathrm{e}}/2L}^{h_{\mathrm{e}}/2L+h_{\mathrm{p}}/L}\frac{\partial\bar{u}^i_{\mathrm{p}}}{\partial\bar{z}}\frac{\partial\bar{w}^j_{\mathrm{p}}}{\partial\bar{x}}\,\mathrm{d}\bar{z}\,\mathrm{d}\bar{x}\right)$$
$$\left.+\frac{e_{31}V}{EL}C^j_{\varphi_{\mathrm{p}}}\int_{h_{\mathrm{e}}/2L}^{h_{\mathrm{e}}/2L+h_{\mathrm{p}}/L}\left(\bar{u}^i_{\mathrm{p}}\Big|_{\bar{x}=-0.5}^{\bar{x}=0.5}\right)\frac{\partial\bar{\varphi}^j_{\mathrm{p}}}{\partial\bar{z}}\,\mathrm{d}\bar{z}\right]+\frac{e_{31}V}{Eh_{\mathrm{p}}}\int_{h_{\mathrm{e}}/2L}^{h_{\mathrm{e}}/2L+h_{\mathrm{p}}/L}\left(\bar{u}^i_{\mathrm{p}}\Big|_{\bar{x}=-0.5}^{\bar{x}=0.5}\right)\mathrm{d}\bar{z}\right\},$$

$$\frac{\partial U_{\mathrm{p}}}{\partial C^i_{w_{\mathrm{p}}}} = bL^2E\left\{\sum_{j=1}^{m}\left[\frac{c_{13}}{E}\left(\frac{h_{\mathrm{e}}}{2L}C^j_{\theta_{\mathrm{e}}}\int_{-0.5}^{0.5}\left(\bar{w}^i_{\mathrm{p}}\Big|_{\bar{z}=h_{\mathrm{e}}/2L}^{\bar{z}=h_{\mathrm{e}}/2L+h_{\mathrm{p}}/L}\right)\frac{\partial\theta^j_{\mathrm{e}}}{\partial\bar{x}}\,\mathrm{d}\bar{x}+C^j_{u_{\mathrm{p}}}\int_{-0.5}^{0.5}\int_{h_{\mathrm{e}}/2L}^{h_{\mathrm{e}}/2L+h_{\mathrm{p}}/L}\frac{\partial\bar{w}^i_{\mathrm{p}}}{\partial\bar{z}}\frac{\partial\bar{u}^j_{\mathrm{p}}}{\partial\bar{x}}\,\mathrm{d}\bar{z}\,\mathrm{d}\bar{x}\right)\right.\right.$$
$$+\frac{c_{33}}{E}C^j_{w_{\mathrm{p}}}\int_{-0.5}^{0.5}\int_{h_{\mathrm{e}}/2L}^{h_{\mathrm{e}}/2L+h_{\mathrm{p}}/L}\frac{\partial\bar{w}^i_{\mathrm{p}}}{\partial\bar{z}}\frac{\partial\bar{w}^j_{\mathrm{p}}}{\partial\bar{z}}\,\mathrm{d}\bar{z}\,\mathrm{d}\bar{x}+\frac{c_{55}}{E}\left(C^j_{u_{\mathrm{p}}}\int_{-0.5}^{0.5}\int_{h_{\mathrm{e}}/2L}^{h_{\mathrm{e}}/2L+h_{\mathrm{p}}/L}\frac{\partial\bar{w}^i_{\mathrm{p}}}{\partial\bar{x}}\frac{\partial\bar{u}^j_{\mathrm{p}}}{\partial\bar{z}}\,\mathrm{d}\bar{z}\,\mathrm{d}\bar{x}\right.\right.$$
$$\left.+C^j_{w_{\mathrm{e}}}\int_{-0.5}^{0.5}\int_{h_{\mathrm{e}}/2L}^{h_{\mathrm{e}}/2L+h_{\mathrm{p}}/L}\frac{\partial\bar{w}^i_{\mathrm{p}}}{\partial\bar{x}}\,\mathrm{d}\bar{z}\frac{\partial\bar{w}^j_{\mathrm{e}}}{\partial\bar{x}}\,\mathrm{d}\bar{x}+C^j_{w_{\mathrm{p}}}\int_{-0.5}^{0.5}\int_{h_{\mathrm{e}}/2L}^{h_{\mathrm{e}}/2L+h_{\mathrm{p}}/L}\frac{\partial\bar{w}^i_{\mathrm{p}}}{\partial\bar{x}}\frac{\partial\bar{w}^j_{\mathrm{p}}}{\partial\bar{x}}\,\mathrm{d}\bar{z}\,\mathrm{d}\bar{x}\right)$$
$$\left.+\frac{e_{33}V}{EL}C^j_{\varphi_{\mathrm{p}}}\int_{h_{\mathrm{e}}/2L}^{h_{\mathrm{e}}/2L+h_{\mathrm{p}}/L}\int_{-0.5}^{0.5}\frac{\partial\bar{w}^i_{\mathrm{p}}}{\partial\bar{z}}\,\mathrm{d}\bar{x}\frac{\partial\bar{\varphi}^j_{\mathrm{p}}}{\partial\bar{z}}\,\mathrm{d}\bar{z}\right]+\frac{e_{33}V}{Eh_{\mathrm{p}}}\int_{-0.5}^{0.5}\left(\bar{w}^i_{\mathrm{p}}\Big|_{\bar{z}=h_{\mathrm{e}}/2L}^{\bar{z}=h_{\mathrm{e}}/2L+h_{\mathrm{p}}/L}\right)\mathrm{d}\bar{x}\right\},$$

$$\frac{\partial U_{\mathrm{p}}}{\partial C^i_{\varphi_{\mathrm{p}}}} = bL^2E\left\{\sum_{j=1}^{m}\left[\frac{e_{31}V}{EL}\left(C^j_{u_{\mathrm{p}}}\int_{h_{\mathrm{e}}/2L}^{h_{\mathrm{e}}/2L+h_{\mathrm{p}}/L}\frac{\partial\bar{\varphi}^i_{\mathrm{p}}}{\partial\bar{z}}\left(\bar{u}^j_{\mathrm{p}}\Big|_{\bar{x}=-0.5}^{\bar{x}=0.5}\right)\mathrm{d}\bar{z}\right)+\frac{e_{33}V}{EL}C^j_{w_{\mathrm{p}}}\int_{h_{\mathrm{e}}/2L}^{h_{\mathrm{e}}/2L+h_{\mathrm{p}}/L}\frac{\partial\bar{\varphi}^i_{\mathrm{p}}}{\partial\bar{z}}\int_{-0.5}^{0.5}\frac{\partial\bar{w}^j_{\mathrm{p}}}{\partial\bar{z}}\,\mathrm{d}\bar{x}\,\mathrm{d}\bar{z}\right.\right.$$
$$\left.\left.-\frac{k_{33}V^2}{EL^2}C^j_{\varphi_{\mathrm{p}}}\int_{h_{\mathrm{e}}/2L}^{h_{\mathrm{e}}/2L+h_{\mathrm{p}}/L}\frac{\partial\bar{\varphi}^i_{\mathrm{p}}}{\partial\bar{z}}\frac{\partial\bar{\varphi}^j_{\mathrm{p}}}{\partial\bar{z}}\,\mathrm{d}\bar{z}\right]-\frac{k_{33}V^2}{ELh_{\mathrm{p}}}nt^{h_{\mathrm{e}}/2L+h_{\mathrm{p}}/L}_{h_{\mathrm{e}}/2L}\frac{\partial\bar{\varphi}^i_{\mathrm{p}}}{\partial\bar{z}}\,\mathrm{d}\bar{z}\right\}.$$

Hence, the elements of the stiffness matrix in Eq. (30) are

$$k^{ij}_{\theta_{\mathrm{e}}\theta_{\mathrm{e}}} = \frac{h_{\mathrm{e}}^3}{12L^3}\int_{-0.5}^{0.5}\frac{\partial\theta^i_{\mathrm{e}}}{\partial\bar{x}}\frac{\partial\theta^j_{\mathrm{e}}}{\partial\bar{x}}\,\mathrm{d}\bar{x}+\frac{\kappa^2G}{E}\frac{h_{\mathrm{e}}}{L}\int_{-0.5}^{0.5}\theta^i_{\mathrm{e}}\theta^j_{\mathrm{e}}\,\mathrm{d}\bar{x}+\frac{c_{11}}{4E}\frac{h_{\mathrm{e}}^2}{L^2}\frac{h_{\mathrm{p}}}{L}\int_{-0.5}^{0.5}\frac{\partial\theta^i_{\mathrm{e}}}{\partial\bar{x}}\frac{\partial\theta^j_{\mathrm{e}}}{\partial\bar{x}}\,\mathrm{d}\bar{x},$$

$$k^{ij}_{\theta_e w_e} = \frac{\kappa^2 G}{E}\frac{h_e}{L}\int_{-0.5}^{0.5}\theta^i_e\frac{\partial \bar{w}^j_e}{\partial \bar{x}}\,d\bar{x},$$

$$k^{ij}_{\theta_e u_p} = \frac{c_{11}}{E}\frac{h_e}{2L}\int_{-0.5}^{0.5}\frac{\partial \theta^i_e}{\partial \bar{x}}\int_{h_e/2L}^{h_e/2L+h_p/L}\frac{\partial \bar{u}^j_p}{\partial \bar{x}}\,d\bar{z}\,d\bar{x},$$

$$k^{ij}_{\theta_e w_p} = \frac{c_{13}}{E}\frac{h_e}{2L}\int_{-0.5}^{0.5}\frac{\partial \theta^i_e}{\partial \bar{x}}\int_{h_e/2L}^{h_e/2L+h_p/L}\frac{\partial \bar{w}^j_p}{\partial \bar{z}}\,d\bar{z}\,d\bar{x} = \frac{c_{13}}{E}\frac{h_e}{2L}\int_{-0.5}^{0.5}\frac{\partial \theta^i_e}{\partial \bar{x}}\left(\bar{w}^j_p\Big|_{\bar{z}=h_e/2L}^{\bar{z}=h_e/2L+h_p/L}\right)d\bar{x},$$

$$k^{ij}_{\theta_e \varphi_u} = 0,$$

$$k^{ij}_{w_e \theta_e} = \frac{\kappa^2 G}{E}\frac{h_e}{L}\int_{-0.5}^{0.5}\frac{\partial \bar{w}^i_e}{\partial \bar{x}}\theta^j_e\,d\bar{x},$$

$$k^{ij}_{w_e w_e} = \frac{\kappa^2 G}{E}\frac{h_e}{L}\int_{-0.5}^{0.5}\frac{\partial \bar{w}^i_e}{\partial \bar{x}}\frac{\partial \bar{w}^j_e}{\partial \bar{x}}\,d\bar{x} + \frac{c_{55}}{E}\frac{h_p}{L}\int_{-0.5}^{0.5}\frac{\partial \bar{w}^i_e}{\partial \bar{x}}\frac{\partial \bar{w}^j_e}{\partial \bar{x}}\,d\bar{x},$$

$$k^{ij}_{w_e u_p} = \frac{c_{55}}{E}\int_{-0.5}^{0.5}\frac{\partial \bar{w}^i_e}{\partial \bar{x}}\int_{h_e/2L}^{h_e/2L+h_p/L}\frac{\partial \bar{u}^j_p}{\partial \bar{z}}\,d\bar{z}\,d\bar{x} = \frac{c_{55}}{E}\int_{-0.5}^{0.5}\frac{\partial \bar{w}^i_e}{\partial \bar{x}}\left(\bar{u}^j_p\Big|_{\bar{z}=h_e/2L}^{\bar{z}=h_e/2L+h_p/L}\right)d\bar{x},$$

$$k^{ij}_{w_e w_p} = \frac{c_{55}}{E}\int_{-0.5}^{0.5}\frac{\partial \bar{w}^i_e}{\partial \bar{x}}\int_{h_e/2L}^{h_e/2L+h_p/L}\frac{\partial \bar{w}^j_p}{\partial \bar{x}}\,d\bar{z}\,d\bar{x},$$

$$k^{ij}_{w_e \varphi_u} = 0,$$

$$k^{ij}_{u_p \theta_e} = \frac{c_{11}}{E}\frac{h_e}{2L}\int_{-0.5}^{0.5}\int_{h_e/2L}^{h_e/2L+h_p/L}\frac{\partial \bar{u}^i_p}{\partial \bar{x}}\,d\bar{z}\frac{\partial \theta^j_e}{\partial \bar{x}}\,d\bar{x},$$

$$k^{ij}_{u_p w_e} = \frac{c_{55}}{E}\int_{-0.5}^{0.5}\int_{h_e/2L}^{h_e/2L+h_p/L}\frac{\partial \bar{u}^i_p}{\partial \bar{z}}\,d\bar{z}\frac{\partial \bar{w}^j_e}{\partial \bar{x}}\,d\bar{x} = \frac{c_{55}}{E}\int_{-0.5}^{0.5}\left(\bar{u}^i_{pu}\Big|_{\bar{z}=h_e/2L}^{\bar{z}=h_e/2L+h_p/L}\right)\frac{\partial \bar{w}^j_e}{\partial \bar{x}}\,d\bar{x},$$

$$k^{ij}_{u_p u_p} = \frac{c_{11}}{E}\int_{-0.5}^{0.5}\int_{h_e/2L}^{h_e/2L+h_p/L}\frac{\partial \bar{u}^i_p}{\partial \bar{x}}\frac{\partial \bar{u}^j_p}{\partial \bar{x}}\,d\bar{z}\,d\bar{x} + \frac{c_{55}}{E}\int_{-0.5}^{0.5}\int_{h_e/2L}^{h_e/2L+h_p/L}\frac{\partial \bar{u}^i_p}{\partial \bar{z}}\frac{\partial \bar{u}^j_p}{\partial \bar{z}}\,d\bar{z}\,d\bar{x},$$

$$k^{ij}_{u_p w_p} = \frac{c_{13}}{E}\int_{-0.5}^{0.5}\int_{h_e/2L}^{h_e/2L+h_p/L}\frac{\partial \bar{u}^i_p}{\partial \bar{x}}\frac{\partial \bar{w}^j_p}{\partial \bar{z}}\,d\bar{z}\,d\bar{x} + \frac{c_{55}}{E}\int_{-0.5}^{0.5}\int_{h_e/2L}^{h_e/2L+h_p/L}\frac{\partial \bar{u}^i_p}{\partial \bar{z}}\frac{\partial \bar{w}^j_p}{\partial \bar{x}}\,d\bar{z}\,d\bar{x},$$

$$k^{ij}_{u_p \varphi_p} = \frac{e_{31}V}{EL}\int_{h_e/2L}^{h_e/2L+h_p/L}\int_{-0.5}^{0.5}\frac{\partial \bar{u}^i_p}{\partial \bar{x}}\,d\bar{x}\frac{\partial \bar{\varphi}^j_p}{\partial \bar{z}}\,d\bar{z} = \frac{e_{31}V}{EL}\int_{h_e/2L}^{h_e/2L+h_p/L}\left(\bar{u}^i_p\Big|_{\bar{x}=-0.5}^{\bar{x}=0.5}\right)\frac{\partial \bar{\varphi}^j_p}{\partial \bar{z}}\,d\bar{z},$$

$$k^{ij}_{w_p \theta_e} = \frac{c_{13}}{E}\frac{h_e}{2L}\int_{-0.5}^{0.5}\int_{h_e/2L}^{h_e/2L+h_p/L}\frac{\partial \bar{w}^i_p}{\partial \bar{z}}\,d\bar{z}\frac{\partial \theta^j_e}{\partial \bar{x}}\,d\bar{x} = \frac{c_{13}}{E}\frac{h_e}{2L}\int_{-0.5}^{0.5}\left(\bar{w}^j_p\Big|_{\bar{z}=h_e/2L}^{\bar{z}=h_e/2L+h_p/L}\right)\frac{\partial \theta^j_e}{\partial \bar{x}}\,d\bar{x},$$

$$k^{ij}_{w_p w_e} = \frac{c_{55}}{E}\int_{-0.5}^{0.5}\int_{h_e/2L}^{h_e/2L+h_p/L}\frac{\partial \bar{w}^i_p}{\partial \bar{x}}\,d\bar{z}\frac{\partial \bar{w}^j_e}{\partial \bar{x}}\,d\bar{x},$$

$$k^{ij}_{w_p u_p} = \frac{c_{13}}{E}\int_{-0.5}^{0.5}\int_{h_e/2L}^{h_e/2L+h_p/L} \frac{\partial \bar{w}^i_p}{\partial \bar{z}}\frac{\partial \bar{u}^j_p}{\partial \bar{x}}\,d\bar{z}\,d\bar{x} + \frac{c_{55}}{E}\int_{-0.5}^{0.5}\int_{h_e/2L}^{h_e/2L+h_p/L} \frac{\partial \bar{w}^i_p}{\partial \bar{x}}\frac{\partial \bar{u}^j_p}{\partial \bar{z}}\,d\bar{z}\,d\bar{x},$$

$$k^{ij}_{w_p w_p} = \frac{c_{33}}{E}\int_{-0.5}^{0.5}\int_{h_e/2L}^{h_e/2L+h_p/L} \frac{\partial \bar{w}^i_p}{\partial \bar{z}}\frac{\partial \bar{w}^j_p}{\partial \bar{z}}\,d\bar{z}\,d\bar{x} + \frac{c_{55}}{E}\int_{-0.5}^{0.5}\int_{h_e/2L}^{h_e/2L+h_p/L} \frac{\partial \bar{w}^i_p}{\partial \bar{x}}\frac{\partial \bar{w}^j_p}{\partial \bar{x}}\,d\bar{z}\,d\bar{x},$$

$$k^{ij}_{w_p \varphi_p} = \frac{e_{33}V}{EL}\int_{h_e/2L}^{h_e/2L+h_p/L}\int_{-0.5}^{0.5} \frac{\partial \bar{w}^i_p}{\partial \bar{z}}\,d\bar{x}\frac{\partial \bar{\varphi}^j_p}{\partial \bar{z}}\,d\bar{z},$$

$$k^{ij}_{\varphi_p \theta_e} = 0,$$

$$k^{ij}_{\varphi_p w_e} = 0,$$

$$k^{ij}_{\varphi_p u_p} = \frac{e_{31}V}{EL}\int_{h_e/2L}^{h_e/2L+h_p/L} \frac{\partial \bar{\varphi}^i_p}{\partial \bar{z}}\int_{\bar{x}_1}^{\bar{x}_2} \frac{\partial \bar{u}^j_p}{\partial \bar{x}}\,d\bar{x}d\bar{z} = \frac{e_{31}V}{EL}\int_{h_e/2L}^{h_e/2L+h_p/L} \frac{\partial \bar{\varphi}^i_p}{\partial \bar{z}}\left(\bar{u}^j_p\Big|_{\bar{x}=-0.5}^{\bar{x}=0.5}\right)d\bar{z},$$

$$k^{ij}_{\varphi_p w_p} = \frac{e_{33}V}{EL}\int_{h_e/2L}^{h_e/2L+h_p/L} \frac{\partial \bar{\varphi}^i_p}{\partial \bar{z}}\int_{-0.5}^{0.5} \frac{\partial \bar{w}^j_p}{\partial \bar{z}}\,d\bar{x}\,d\bar{z},$$

$$k^{ij}_{\varphi_p \varphi_p} = -\frac{k_{33}V^2}{EL^2}\int_{h_e/2L}^{h_e/2L+h_p/L} \frac{\partial \bar{\varphi}^i_p}{\partial \bar{z}}\frac{\partial \bar{\varphi}^j_p}{\partial \bar{z}}\,d\bar{z}$$

and elements of the external load vector are

$$t_1 = -\frac{h_e}{2L}\frac{e_{31}V}{EL}\int_{-0.5}^{0.5}\frac{\partial \theta^i_e}{\partial \bar{x}}\,d\bar{x} = -\frac{h_e}{2L}\frac{e_{31}V}{EL}\left(\theta^i_e\Big|_{\bar{x}=-0.5}^{\bar{x}=0.5}\right),$$

$$t_2 = 0,$$

$$t_3 = -\frac{e_{31}V}{Eh_p}\int_{-0.5}^{0.5}\int_{h_e/2L}^{h_e/2L+h_p/L}\frac{\partial \bar{u}^i_p}{\partial \bar{x}}\,d\bar{z}\,d\bar{x} = -\frac{e_{31}V}{Eh_p}\int_{h_e/2L}^{h_e/2L+h_p/L}\left(\bar{u}^i_p\Big|_{\bar{x}=-0.5}^{\bar{x}=0.5}\right)d\bar{z},$$

$$t_4 = -\frac{e_{33}V}{Eh_p}\int_{-0.5}^{0.5}\int_{h_e/2L}^{h_e/2L+h_p/L}\frac{\partial \bar{w}^i_p}{\partial \bar{z}}\,d\bar{z}\,d\bar{x} = -\frac{e_{33}V}{Eh_p}\int_{-0.5}^{0.5}\left(\bar{w}^i_p\Big|_{\bar{z}=h_e/2L}^{\bar{z}=h_e/2L+h_p/L}\right)d\bar{x},$$

$$t_5 = 0.$$

References

ABAQUS/Explicit User's Manual, Version 6.3, Habbit, Karlsson & Sorensen, Inc., USA, 2002.

Batra, R.C., Liang, X.Q., Yang, J.S., 1996a. Shape control of vibrating simply supported rectangular plates. AIAA J. 34, 116–122.

Batra, R.C., Liang, X.Q., Yang, J.S., 1996b. The vibration of a simply supported rectangular elastic plates due to piezoelectric actuators. Int. J. Solids Struct. 33, 1597–1618.

Cady, W.G., 1964. Piezoelectricity. Dover Pub., New York.

Cheng, Z.Q., Lim, C.W., Kitipornchai, S., 1999. Three-dimensional exact solution for inhomogeneous and laminated piezoelectric plates. Int. J. Eng. Sci. 37 (11), 1425–1439.

Cheng, Z.Q., Lim, C.W., Kitipornchai, S., 2000. Three-dimensional asymptotic approach to inhomogeneous and laminated piezoelectric plates. Int. J. Solids Struct. 37 (23), 3153–3175.

Cheng, Z.Q., Reddy, J.N., 2002. Asymptotic theory for laminated piezoelectric circular cylindrical shells. AIAA J. 40 (3), 553–558.

Crawley, E.F., Anderson, E.H., 1990. Detailed models of piezoceramic actuation beams. J. Intell. Mater. Syst. Struct. 1, 4–25.

Crawley, E.F., de Luis, J., 1987. Use of piezoelectric actuators as elements of intelligent structures. AIAA J. 25 (10), 1373–1385.

Crawley, E.F., Lazarus, K.B., 1991. Induced strain actuation of isotropic and anisotropic plates. AIAA J. 29 (6), 944–951.

He, L.H., Lim, C.W., 2003. Electromechanical responses of piezoelectric fiber composites with sliding interface under anti-plane deformations. Composites Part B: Eng. 34 (4), 373–381.

He, L.H., Lim, C.W., Soh, A.K., 2000. Three-dimensional analysis of an antiparallel piezoelectric bimorph. Acta Mech. 145 (1–4), 189–204.

Huang, D., Sun, B., 2001. Approximate analytical solutions of smart composite Mindlin beams. J. Sound Vib. 244, 379–394.

Kapuria, S., Dumir, P.C., Ahmed, A., 2003a. An efficient coupled layerwise theory for static analysis of piezoelectric sandwich beams. Arch. Appl. Mech. 73 (3–4), 147–159.

Kapuria, S., Dumir, P.C., Ahmed, A., 2003b. An efficient higher order zigzag theory for composite and sandwich beams subjected to thermal loading. Int. J. Solids Struct. 40 (24), 6613–6631.

Kapuria, S., Dumir, P.C., Ahmed, A., 2003c. An efficient coupled layerwise theory for dynamic analysis of piezoelectric composite beams. J. Sound Vib. 261 (5), 927–944.

Kapuria, S., Dumir, P.C., Ahmed, A., 2004a. Efficient coupled zigzag theory—for hybrid piezoelectric beams for thermoelectric load. AIAA J. 42 (2), 383–394.

Kapuria, S., Dumir, P.C., Jain, N.K., 2004b. Assessment of zigzag theory for static loading, buckling, free and forced response of composite and sandwich beams. Comp. Struct. 64 (3–4), 317–327.

Koconis, D.B., Kollár, L.P., Springer, G.S., 1994a. Shape control of composite plates and shells with embedded actuators. I. Voltages specified. J. Compos. Mater. 28, 415–458.

Koconis, D.B., Kollár, L.P., Springer, G.S., 1994b. Shape control of composite plates and shells with embedded actuators. II. Desired shape specified. J. Compos. Mater. 28, 459–482.

Lee, C.K., 1990. Theory of laminated piezoelectric plates for the design of distributed sensors/actuators. Part I: Governing equations and reciprocal relationships. J. Acoust. Soc. Am. 87, 1144–1158.

Lee, C.K., Moon, F.C., 1989. Laminated piezopolymer plates for torsion and bending sensors and actuators. J. Acoust. Soc. Am. 85, 2432–2439.

Liew, K.M., Liang, J., 2003. Three-dimensional piezoelectric boundary element analysis of transversely isotropic half-space. Comput. Mech. 32 (1–2), 29–39.

Liew, K.M., Sivashanker, S., He, X.Q., Ng, T.Y., 2003. The modelling and design of smart structures using functionally graded materials and piezoelectrical sensor/actuator patches. Smart Mater. Struct. 12 (4), 647–655.

Lim, C.W., He, L.H., 2001. Exact solution of a compositionally graded piezoelectric layer under uniform stretch, bending and twisting. Int. J. Mech. Sci. 43 (11), 2479–2492.

Lim, C.W., He, L.H., 2004. Three-dimensional exact solutions for electro-mechanical response of triple-layer piezoelectric actuators. Smart Mater. Struct. 13, 1050–1058.

Lim, C.W., He, L.H., Soh, A.K., 2001. Three dimensional electromechanical responses of a parallel piezoelectric bimorph. Int. J. Solids Struct. 38 (16), 2833–2849.

Lin, Q., Jin, Z., Liu, Z., 2000. An analytical solution to the laminated piezoelectric beam under the electric field. Struct. Eng. Mech. 10, 289–298.

Luo, Q., Tong, L., 2002. Exact static solutions to piezoelectric smart beams including peel stresses. Part I: Theoretical formulation. Int. J. Solids Struct. 39, 4677–4695.

Mason, W.P., 1981. Piezoelectricity, its history and applications. J. Acoust. Soc. Am. 70, 1561–1566.

Meguid, S.A., Chen, Z.T., 2001. Transient response of a finite piezoelectric strip containing coplanar insulating cracks under electromechanical impact. Mech. Mater. 33 (2), 85–96.

Meguid, S.A., Zhao, X., 2002. The interface crack problem of bonded piezoelectric and elastic half-space under transient electromechanical loads. J. Appl. Mech. ASME 69 (3), 244–253.

Mindlin, R.D., 1951. Influence of rotatory inertia and shear on flexural motion of isotropic, elastic plates. J. Appl. Mech. ASME 18, 31–38.

Mitchell, J.A., Reddy, J.N., 1995. A refined hybrid plate-theory for composite laminates with piezoelectric laminae. Int. J. Solids Struct. 32 (16), 2345–2367.

Nye, J.F., 1976. Physical Properties of Crystal and Their Representation by Tensors and Matrix. Oxford University Press, Oxford.

Reddy, J.N., 1984. Energy and Variational Methods in Applied Mechanics: with an Introduction to the Finite Element Method. Wiley Interscience.

Reddy, J.N., Mitchell, J.A., 1995. On refined nonlinear theories of laminated composite structures with piezoelectric laminae. Sadhana-Acad. P Eng. S 20, 721–747 (Parts 2–4).

Reissner, E., 1945. The effect of transverse shear deformation on the bending of elastic plates. J. Appl. Mech. ASME 12, A69–A77.
Saravanos, D.A., Heyliger, P.R., 1995. Coupled layerwise analysis of composite beams with embedded piezoelectric sensors and actuators. J. Intell. Syst. Struct. 6 (3), 350–363.
Shen, H.-S., 2001. Postbuckling of shear deformable laminated plates with piezoelectric actuators under complex loading conditions. Int. J. Solids Struct. 38 (44–45), 7703–7721.
Shen, H.-S., 2002. Postbuckling of laminated cylindrical shells with piezoelectric actuators under combined external pressure and heating. Int. J. Solids Struct. 39 (16), 4271–4289.
Tiersten, H.F., 1969. Linear Piezoelectric Plate Vibrations. Plenum Press, New York.
Tzou, H.S., 1993. Piezoelectric Shells: Distributed Sensing and Control of Continua. Kluwer Academic, Dordrecht.
Tzou, H.S., Gadre, M., 1989. Theoretical analysis of a multi-layered thin shell coupled with piezoelectric shell actuators for distributed vibration controls. J. Sound Vib. 132, 433–450.
Tzou, H.S., Zhong, J.P., 1993. Electromechanics and vibrations of piezoelectric shell distributed systems. J. Dynam. Syst. Measure. Contr. 115, 506–517.
Wang, B.T., Rogers, C.A., 1991. Laminated theory for spatially distributed induced strain actuators. J. Compos. Mater. 25, 433–453.
Wang, Q., Liew, K.M., 2003. Analysis of wave propagation in piezoelectric coupled cylinder affected by transverse shear and rotary inertia. Int. J. Solids Struct. 40 (24), 6653–6667.
Yocum, M., Abramovich, H., 2002. Static behaviour of piezoelectric actuated beam. Comput. Struct. 80, 1797–1808.